Elsevier Editorial System(tm) for Construction & Building Materials
Manuscript Draft

Manuscript Number: CONBUILDMAT-D-19-05302R1

Title: Heating Potential of Aggregates in Asphalt Mixtures Exposed to Microwaves Radiation

Article Type: Research Paper

Keywords: Asphalt Mixture, Microwave assisted-healing, Aggregates, Petrography

Corresponding Author: Mrs. Laura Trigos,

Corresponding Author's Institution: Universidad Politécnica de Madrid

First Author: Laura Trigos

Order of Authors: Laura Trigos; Juan Gallego, PhD; Jose Escavy, PhD

Abstract: Recent studies have shown that microwave energy can repair micro-cracks in asphalt mixtures by heating them. This process may be described as assisted self-healing. Several studies have tested different types of asphalt mixtures with various metallic additions in order to increase the susceptibility to microwaves and consequently the effectiveness of the healing process. Usually, aggregates account for more than 90% in weight of the asphalt mixture, playing an important role in heating efficacy. This is due to the different energy-heating ramps for each type of aggregate giving rise to different temperatures and energy-repair rates. The studies carried out on this subject are scarce and in no case clarify the influence of the aggregate type in terms of microwave susceptibility of asphalt mixtures.
Focusing efforts on this issue would promote a change in the manufacturer's design or repair of asphalt pavements, since it would extend the service life and will greatly reduce the economic and polluting effects, such as the release of greenhouse gases into the atmosphere and the volume of waste from the maintenance of roads.
In this study, by means of different laboratory tests, detailed petrographic, mineralogical, and chemical analyses have been carried out on 10 different aggregates frequently used for pavements construction. Additionally, a procedure has been developed to measure the aggregates heating potential under microwave radiation. Based on the results of the study a classification for aggregates, according to their heating potential under microwaves, is proposed. This classification should be taken into account in order to optimise the asphalt mixture formula and to estimate the energy to be applied to asphalt mixtures for effective assisted self-healing.

Heating Potential of Aggregates in Asphalt Mixtures Exposed to Microwaves Radiation

Laura Trigos[a], Juan Gallego[b], José Ignacio Escavy[a]

a- Departamento de Ingeniería y Morfología del Terreno. ETSICCP. Universidad Politécnica de Madrid. C/ Profesor Aranguren s/n, 28040, Madrid, Spain

b- Departamento de Ingeniería del Transporte, Urbanismo y Territorio. ETSICCP. Universidad Politécnica de Madrid. C/ Profesor Aranguren s/n, 28040, Madrid, Spain

Keywords

Asphalt Mixture, Microwave assisted-healing, Aggregates, Petrography

Highlights

Aggregates are the main constituent of asphalt mixtures

Petrographic and chemical techniques were used to determine aggregates composition

Different aggregates were heated by microwaves

Microwave heating tests on different aggregates gave rise to uneven heating results

A parameter has been proposed to classify aggregates according to the efficiency of the heating process

Graphical Abstract

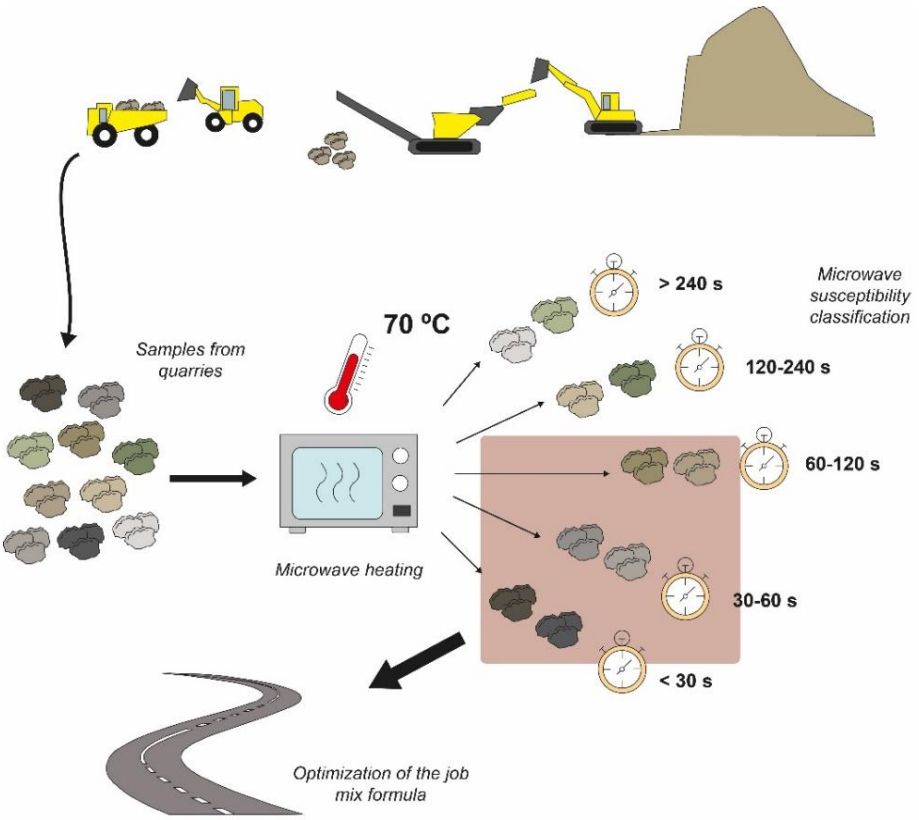

Abstract

Recent studies have shown that microwave energy can repair micro-cracks in asphalt mixtures by heating them. This process may be described as assisted self-healing. Several studies have tested different types of asphalt mixtures with various metallic additions in order to increase the susceptibility to microwaves and consequently the effectiveness of the healing process. Usually, aggregates account for more than 90% in weight of the asphalt mixture, playing an important role in heating efficacy. This is due to the different energy-heating ramps for each type of aggregate giving rise to different temperatures and energy-repair rates. The studies carried out on this subject are scarce and in no case clarify the influence of the aggregate type in terms of microwave susceptibility of asphalt mixtures.

Focusing efforts on this issue would promote a change in the manufacturer's design or repair of asphalt pavements, since it would extend the service life and will greatly reduce the economic and polluting effects, such as the release of greenhouse gases into the atmosphere and the volume of waste from the maintenance of roads.

In this study, by means of different laboratory tests, detailed petrographic, mineralogical, and chemical analyses have been carried out on 10 different aggregates frequently used for pavements construction. Additionally, a procedure has been developed to measure the aggregates heating potential under microwave radiation. Based on the results of the study a classification for aggregates, according to their heating potential under microwaves, is proposed. This classification should be taken into account in order to optimise the asphalt mixture formula and to estimate the energy to be applied to asphalt mixtures for effective assisted self-healing.

1. Introduction

The maintenance of infrastructures, such as asphalt pavements, is of vital importance, since their proper conservation reduces future economic costs and environmental impact. The poor preservation and the premature failure of asphalt pavements cause safety, economic, and environmental problems. Production, transport, and installation of materials produce a high impact, including energy consumption, as well as the emissions of greenhouse gases into the atmosphere [1]. Consequently, an increased service life of the road's pavements, could be a key factor to reduce these social costs.

Over the last few years, the concept of *"self-healing"* has been introduced to extend the service life of asphalt pavements. This process was initially mentioned in the 1960s by Bazin and Saunier [2]and it has been widely studied from then till the present day. It deals with the reparation of micro-cracks , that develop in the asphalt mixtures by the action of traffic loads and weather conditions on the pavements [3].

Self-healing consists in the recovery of initial properties such as the dynamic modulus. In bituminous materials it usually refers to the reduction of micro-cracks found in the pavement [4]. The main mechanisms of recovery are wetting of the micro-cracks edges and diffusion of the souronding bitumen that results in the closure of cracks by the surface tension of the bitumen and the aleatory dissemination of the bitumen [5].

Studies carried out on this matter suggest that self-healing occurs without intervention. Other authors [3,6]mention that the only hindrance for non-assisted healing is long periods of rest needed for an effective repair of the cracks. Another factor to be considered is temperature. Different authors [3,7–10]have determined that the temperature at which the process begins ranges from 30 ^{o}C to 70 ^{o}C. The temperature for self-healing in asphalt mixtures can vary depending on the type of mixture and rest periods given to the pavement [6,8–14].

In order to overcome the long periods of rest and temperature, assisted heating techniques such as active warming (applied or induced) were developed. Techniques such as induction heating [3,8,15,16], infrared heating, [17] or microwave heating [3,6,12,15,17–21] have been tested. This article focuses on asphalt repair by microwave as the assisted heating technique.

The microwave treatment has demonstrated its energy efficiency compared to other techniques and is less harmful to the asphalt mixture when compared with infrared heating [12,17,22]. In addition, the use of microwaves is already a widely used technique in different industrial applications [22–24]. The most important benefits are the in situ non-emission of polluting gases, higher heating rate that translates to energy savings, and the reduction of risks for the operators [25].

To understand how microwave heating occurs, the first consideration is to comprehend the way in which the microwaves interact with matter. Microwaves are non-ionising electromagnetic radiation [22,23]. The waves cause heating of the matter by oscillation, rotation, or vibrations of molecules. As the energy is transmitted to the particles, the heat is generated from within the material. This type of heating is known as volumetric heating [12,22,26]. It should also be taken into consideration that the characteristics of the material affect the heating, therefore, materials are classified into three groups according to their affinity with microwaves: a) insulating or transparent, b) conductor or metallic, and c) absorbent or dielectric [12].

There are many studies where healing of asphalts is studied through the application of microwave radiation. In these studies, the topic of warming is approached from different perspectives, most of them regarding the addition of new components to the mixture. The use of additions, usually metallic components, such as steel slags [27],

metallic fibres [15,21], steel wool [6,21,28,29], or iron powders [12,14] has been tested in order to improve the susceptibility to microwaves as well as to maximise the thermal conductivity of the mixture. On the other hand, there are few studies that focus on the aggregates behaviour, although recent studies on microwave assisted-healing in asphalt mixtures [29,30] aim to increase the research on the aggregates. Regarding the microwave heating of aggregates, it is important to mention the work of Benedetto and Calvi [25] who studied the heating of two different aggregates (basalt and siliceous-calcareous gravel) to check if they present differential heating. The results of the work proved the differential heating between different lithologies. In this paper, a similar methodology will be developed, introducing new lithologies of aggregates that were not studied, in order to understand the relation between microwave heating behaviour and the petrology of the aggregates.

The study of the aggregates behaviour in the asphalt mix under microwave radiation is of great interest since aggregates account for more than 90% by weight of the asphalt mix [31]. Fortes *et al.* [32] studied the aggregates used in road construction, pointing out the need for an appropriate combination of characteristics (mechanical properties, shape or gradation) contributing to the performance of the mixture.

In the 70's, a technical experience of microwave-assisted repair was carried out with a mobile device equipped with microwaves, providing promising results, but the lack of awareness about the sustainable use of resources caused this technology not to be developed [33]. At present, mobile prototypes equipped with microwaves have been developed to remove ice sheets [34,35]. One of the aims of this work is to identify the aggregates which present better rates of heating in order to make the microwave-assisted healing technique more energy efficient. For this reason, a set of commonly-used aggregates in asphalt mixtures have been chosen. Most of the aggregates selected for this study can be found in Spain, but some of the lithologies chosen are rare in this country [36], these less common samples have been collected from other countries, such as Chile and Brazil. Mono-lithological aggregates were selected to avoid the formation of heterogeneous heating due to the formation of micro-plasmas or hot spots [22] that would cause cracking due to selective heating [22,37].

The optimal heating temperature will be determined, to find out at which temperature ranges healing occurs and the optimal temperatures to avoid aging of the bitumen. Depending on the type of bitumen, resting time, and technique used, the temperature at which the healing process begins is variable, starting between 30 ^{o}C and 70 ^{o}C [9]. It is known that higher heating temperatures increase the recovery of stiffness modulus. García *et al.* [7] tested the bitumen, observing that at temperatures below 100 ^{o}C there is no premature aging. With respect to the optimal heating temperature, there are also discrepancies, Zhu *et al.* [14] determined that the optimum temperature is 55 ^{o}C when a resting time of 3h is provided. In the same way, Liu *et al.* [13] established the optimum temperature at 85 ^{o}C with a resting time of between 1-2h.

The objective of the study is to analyse the influence of aggregates in the asphalt mix heating. Ten aggregates were studied to find out the potential heating causes. For this reason, a series of studies were carried out to characterise the rocks (petrographic, mineralogical, and chemical characterisation)., then a heating test was developed based on the work of Benedetto and Calvi [25]. In the seminal work of Benedetto and Calvi [25] only two aggregate types (basalt and siliceous-calcareous) were studied and only their chemistry was determined. It has been considered necessary to increase the number and type of aggregates together with the type of analysis in order to better define the impact of the aggregates in the microwave assisted-healing process.

2. Materials and Methods

2.1. Materials

Ten samples of different natural and artificial aggregate types were considered in this study. These were collected from different quarries around Spain, Chile and Brazil. The selected aggregates are commonly employed for roads construction [32,38,39]. Their composition is diverse, and they have been classified into four groups according to their composition and origin (Table 1). In this way it is possible to compare the efficiency of heating by microwaves based on their different textures, as well as mineralogical and chemical compositions. To avoid the influence of particle size during

the heating process, the rocks were crushed and sieved to ensure a similar particle size (fraction 4/8 mm).

Table 1
Samples of aggregates studied and their classification according to their genetic origin.

Group	Sample	Agreggate	Ranking
1	BFS-1	Blast-furnace slag	Steelmaking waste
	BFS-2	Blast-furnace slag	
2	CAL-1	Limestone	Calcareous sedimentary rocks
	DOL-1	Dolostone	
3	QRT-1	Quartzite river gravel	Metamorphic quartzite rocks
	QRT-2	Quartzite	
4	OPH-1	Ophite	Igneous rocks and mixture of igneous and metamorphic rocks
	AND-1	Andesite	
	AND-2	Andesite and others	
	MTS-1	Metasandstone and others	

2.2. Petrographic analysis and compositional characterisation

For the petrographic study and the mineralogical and chemical characterisation, different tests have been performed. First, a macroscopic and microscopic description was carried out with optical microscopy of transmitted light (OM), both included in the EN 12407 standard (Natural stone test methods) [40]. In addition, for mineralogical and chemical characterisation, X-ray diffraction (XRD) and X-ray fluorescence (XRF) was used.

For the macroscopic description, a hand magnifying lens (x15) was used to define the main minerals, their shape, colour and size, etc. For the microscopic characterisation, 30 µm-thick thin sections were used. Samples corresponding to carbonates were stained with Alizarin red-S to distinguish between calcite and dolomite. During the study, a semi-quantitative estimation by point-counting of the different observed components in the Petrographic Microscope was made. Petrographic characterisation was performed using a Zeiss West Germany Optical 316 Microscope with 2.5x, 10x and 40x magnifications, with transmitted and polarised light sources, in the Department of Mineralogy and Petrology at the Complutense University of Madrid.

Bulk mineralogy was determined by X-ray diffraction (XRD). A portion of the samples was ground in an agate mortar to obtain a 53 µm powder. Non-oriented powder was examined on a Philips PW 1720 diffractometer with Cu (Kα) radiation and a Bruker D8 Advance diffractometer equipped with a Sol-X detector and Cu (Kα) radiation, in the CAI of Geological Techniques (Complutense University of Madrid). The quantification of mineral phases was carried out using the Chung method (1975) [41] by Bruker software (EVA). Finally, X-ray fluorescence (XRF) was performed, using a wavelength dispersive X-ray fluorescence spectrometer (Bruker, S2 Ranger) to obtain a semi-quantitative analysis of the chemical composition of the sample.

2.3. Microwave heating

To study the heating produced by microwave energy on different aggregates, the authors developed an assay protocol that consisted of measuring the heating efficiency of each aggregate under study. The test is based on microwave-radiation application to aggregates with different compositions and mineralogical characteristics, such as the crystal size.

For this test, the size of the aggregates samples were between 4 and 8 mm in order to avoid potential heating differences related to the size of the particles [42]. Before performing the study, the aggregates were washed and dried in an oven at a temperature below 100 ^{o}C.

To maintain a constant temperature in the aggregates, these were introduced in an oven at 22 ^{o}C for 24 hours. Later, a sample of 200g of aggregate was introduced in a polypropylene plastic container. The container has a height of 10 cm and a diameter of 6.5 cm. Plastic containers heated less than glass containers under microwave radiation, limiting the conduction heating of the aggregates due to the container.

In this process, an Orbegozo MI-2014 20L microwave oven was used, with an output power of 700 W and a frequency of 2.45 GHz; maximum power was used during the tests. Measurements of the actual energy consumed were performed with an Efergy EF029 measurement device, logged approximate values of 0.96 KWh. The test consisted in measuring the temperature with an infrared temperature gun (Testo 830-

T1), heating the aggregate at fixed time intervals (every 20 seconds) until the bulk aggregate reached a surface temperature above 110 ^{o}C.

During the design of the experiment, the randomisation principle was followed through the use of random number tables to ensure the independence of the data. The authors repeated the experiment 50 times to avoid the underestimation of the variability. During this process, measurements of the ambient temperature were also taken in case this affected the results. Subsequently, the diagnosis of the data was checked to ensure that they were correct (homoscedasticity, normality, and independence). Finally, the mean, range, and standard deviation were calculated.

3. Results

3.1. Samples characterization

The results of the ten aggregate types examined in this study are summarised in Table 2 (mineral phases obtained by means of XRD) and Table 3 (Chemical data by XRF)

Table 2

Mineral phases obtained by means of XRD for each sample given in percentage. The abbreviations correspond to the following mineral phases: ***Qz*** quartz, ***Plg*** plagioclase group, ***Bt*** biotite, ***Ms*** muscovite, ***Chl*** chlorite, ***Aug*** augite, ***Hbl*** hornblende, Cal calcite, ***Dol*** dolomite, ***Mll*** melilite group, ***Rt*** rutile, ***Grt*** garnet group, ***Prv*** perovskite, ***Mtc*** monticellite, ***Merw*** merwinite and ***Montm*** montmorillonite.

Sample	*Qz*	*Plg*	*Bt*	*Ms*	*Chl*	*Aug*	*Hbl*	*Cal*	*Dol*	*Mll*	*Rt*	*Grt*	*Prv*	*Mtc*	*Merw*	*Montm*
BFS-1	41.4									26.7		19.8			12.2	
BFS-2	8.8									33.2		26.4	3.3	28.3		
CAL-1	1.3							98.7								
DOL-1									100							
QRT-1	100															
QRT-2	100															
OPH-1	9.1	31.8			21	25.2					12.9					
AND-1	18.9	50.7					24.1									6.4
AND-2		45.7	5.7		18.9		29.8									
MTS-1	80.3			5.2	14.4											

Table 3

Chemical data obtained by means of XRF, for each sample given in percentage by weight.

Elemental Component	BFS-1	BFS-2	CAL-1	DOL-1	QRT-1	QRT-2	OPH-1	AND-1	AND-2	MTS-1
SiO_2	18.22	12.42	0.72	0.37	96.09	97.72	45.6	56.38	51.37	61.02
Al_2O_3	11.78	13.06	0.27		2.15	1.51	16.03	18.41	18.54	18.7
Fe_2O_3	24.23	32	0.09	0.17	0.44	0.19	11.14	6.78	8.51	7.51
MgO	3.5	3.7	0.3	17.8	0.2		7.5	3.3	3.4	1.8
MnO	1.41	1.14					0.06	0.05	0.05	0.04
CaO	34.12	29.59	54.64	33.74	0.07		12.66	3.7	6.42	0.46
Na_2O	0.5	0.1		0.7	0.1	0.04	2.6	5	4.8	0.6
K_2O	0.37	0.3	0.41	0.27	0.14		0.54	2.63	2.06	5.55
TiO_2	0.88	0.88			0.1	0.11	1.09	0.86	0.93	1.36
P_2O_5	0.23	0.27						0.13	0.35	
Cr_2O_3	2.47	3.05					0.08			0.01
CO_2	1.8	2.2	43.3	46.7	0.4	0.2	2.1	2.3	3.1	2.4
Others	0.52	1.31	0.21	0.28	0.22	0.2	0.64	0.48	0.38	0.52

For the textural and compositional description, the EN 12407 standard (Natural stone test methods. Petrographic examination) [40] was followed. In addition, the terms used are included in the EN 12670 standard (Natural stone. Terminology) [43]. Regarding organisation; classifications have been adopted according to the genetic origin of rocks. As for igneous rocks (plutonic and volcanic); these were classified according to their modal composition. For this reason, they are projected in the QAPF diagram of Le Maitre [44]. Two classifications are used for the classification of carbonate rocks: Dunham [45]: for rocks of calcitic composition and Friedman [46]: for

rocks with dolomitic composition. Finally, the Eskola method modified by Turner and Verhoogen [47] was used for metamorphic rock classification.

For the description and classification of blast furnace slag, a different methodology was followed. Blast furnace steel slag is the combination of iron ores, coke ash and limestone materials such as lime and magnesia used as fluxes, in different proportions [48]. The combination of all these materials occurs at a high temperature (= 1,600 ^{o}C) [48]. In general, they are formed by vitreous and crystalline phases, although the abundance of the latter depends on the type of cooling, therefore, they are classified according to their content in silicates and the cooling time [49,50]. In addition, they are classified according to their silicate index (ί, Equation 1), where the oxygen content of the silica is divided among other oxides. If the result is greater than 1, it is considered acid; if it is less than 1 is considered basic. If it is equal to one, it is neutral [49].

$$ί = \frac{O\ of\ SiO_2}{O\ of\ the\ Bases} \quad (1)$$

Blast-furnace slag (BFS) BFS-1 sample is a dark-coloured crystallised slag with basic composition (Fig. 1A). It is composed of two phases: vitreous (80%) and crystallised (20%). Under the microscope, the crystalline phase corresponds to medium to fine-grained gehlenite (melilite group) that presents different textures such as dendritic, vacuolar and fibrous. The porosity (<5%) is low (Fig. 2A). The mineralogy obtained with XRD analysis corresponds with gehlenite (melilite group), merwinite, quartz and garnet (Table 2). The chemistry obtained with XRF is shown in Table 3, resulting in values of 34.12% CaO, 24.23% Fe_2O_3, 18.22% SiO_2, 11.78% Al_2O_3, 3.5% MgO, 2.47% Cr_2O_3 and a small proportion of other compounds.

Blast-furnace slag (BFS) BFS-2 is a dark-coloured crystallised slag with basic composition (Fig. 1B). It is also composed of two phases: vitreous (90%) and crystalline (10%). The crystalline phase corresponds to akermanite (melilite group), this crystalline phase has vacuolar texture, the minerals are fine-grained. The porosity is 15% (Fig. 2B).

The mineralogy obtained with XRD analysis corresponds with akermanite (melilite group), monticellite, garnet, quartz and perovskite (Table 2). The chemistry obtained with XRF is shown in the Table 3, resulting in values of 32% Fe_2O_3, 29.59% CaO, 13.06% Al_2O_3, 12.42% SiO_2, 3.7% MgO, 3.05% Cr_2O_3 and a small proportion of other compounds.

Limestone CAL-1 is a carbonate rock of calcitic composition (Fig.1C). It presents depositional texture; but some diagenetic processes such as cementation, neo-morphism, micritisation, recrystallization, and compaction can be observed. According to the Dunham classification, this rock is a Mudstone with ostracods, bivalves, gastropods and peloids. Regarding the diagenetic processes, the types of cement appearing within fossil structures are of the sparitic type with sizes of 0.5 mm. The remains of bivalves have suffered neo-morphism or recrystallisation. The micritisation is possibly caused by a very intense bioturbation process. Slight mechanical compaction can also be observed. There is no presence of porosity (Fig. 2C). The mineralogy obtained with XRD analysis corresponds to calcite and quartz (Table 2). The chemistry obtained with XRF is shown in the Table 3, resulting in a value of 54.64% CaO, 43.3% CO_2 and small a proportion of other compounds.

Dolostone DOL-1 is a carbonate rock of crystalline dolomite composition (Fig. 1D). It does not present depositional texture, and the observed diagenetic processes are dolomitization and porosity formation. It has a microsparite texture, fine to medium crystalline, anhedral and hypidiotopic. Presents 10% of vug type porosity with size <0.5mm (Fig. 2D). The mineralogy obtained with XRD analysis corresponds with dolomite (Table 2). The chemistry obtained with XRF is shown in the Table 3, resulting in values of 46.7% CO2, 33.74% CaO, 17.8% MgO and a small proportion of other compounds.

Quartzite (river-gravel) QRT-1 is composed of pebbles of different compositions (Fig. 1E). The sample under the microscope shows pebbles with different crystal sizes. The most abundant type has fine to coarse grain size and granular texture and accounts for more than 85% of the sample. The rest of the sample (15% of the total) has medium grain and granular texture with undulose extinction. The minerals observed in the thin section are quartz 95% and chlorite 5% (Fig. 2E). The mineralogy obtained with XRD

analysis corresponds to quartz (Table 2). The chemistry obtained with XRF is shown in Table 3, resulting in values of 96.09% SiO_2, 2.15% Al_2O_3 and a small proportion of other compounds.

Quartzite (crushed rock) QRT-2 (Fig. 1F) has medium to coarse grain size and granular texture. The minerals observed in the thin section are quartz (>95%) the rest being chlorite. No special texture is observed, except undulose extinction in the large quartz grains (Fig. 2F). The mineralogy obtained with XRD analysis corresponds to quartz (Table 2). The chemistry obtained with XRF is shown in the Table 3, resulting in values of 97.72% SiO_2, 1.51% Al_2O_3 and traces of other compounds.

Ophite OPH-1 (Fig. 1G) has a holocrystalline, phaneritic, with an equigranular tendency with intergranular texture, and hypidiomorphic fine-medium crystals. Zonation is observed at the edges of the pyroxene crystals, corresponding to an alteration to amphiboles. Regarding the structures, a banded in the sizes of the crystals is observed since these are distributed from 0.2-2mm (Fig. 2G). The mineralogy obtained with XRD analysis corresponds with anorthite, augite, quartz, chlorite, and rutile (Table 2). The chemistry obtained with XRF (Table 3), resulted in values of 45.6% SiO_2, 16.06% Al_2O_3, 12.66% CaO, 11.14% Fe_2O_3, 7.5% MgO, 2.6% Na_2O and a small proportion of other compounds.

Andesite AND-1 (Fig. 1H) has a hypocrystalline, inequigranular porphyritic, medium grain and panidiomorphic texture. The presence of zonation in plagioclase is very abundant. Another zonation is the alteration in the edges of the amphiboles (hornblende) where chlorite is formed (Fig. 2H). The mineralogy obtained with XRD analysis corresponds with albite, hornblende, and quartz (Table 2). The chemistry obtained with XRF is shown in the Table 3, resulting in values of 56.38% SiO_2, 18.41% Al_2O_3, 6.78% Fe_2O_3, 5% Na_2O, 3.7% CaO, 3.3% MgO, 2.63% K_2O and traces of other compounds.

Chile Sample AND-2. This sample is composed of four lithologies (Fig. 1I). Andesite (80%), basalt (10%), quartzite (5%) and mica-schist (5%). Andesite has hypocrystalline, inequigranular porphyritic, medium grain and panidiomorphic texture. Under the microscope, anorthite 40%, hornblende 25% and volcanic glass 40% may be

distinguished. The presence of zonation in plagioclase is abundant. The second is basalt and has a holocrystalline texture, equigranular tendency with an intergranular texture, medium grain and hypidiomorphic. Under the microscope, diopside 80% and anorthite 20% may be observed. The anorthite crystals are being altered to clay minerals. The third lithology corresponds to quartzite, and it has granular texture with fine grain. The mineral observed in the thin section is quartz. The last lithology corresponds to mica-schist has a lepidoblastic texture with fine grain. It presents a banded texture and crenulations. Under the microscope, biotite 85%, quartz 10% and opaque minerals 5% can be distinguished. (Fig. 2I). The mineralogy obtained with XRD analysis corresponds with anorthite, biotite, hornblende, and chlorite (Table 2). The chemistry obtained with XRF is shown in the Table 3, resulting in a value of 51.37% SiO_2, 18.54% Al_2O_3, 8.51% Fe_2O_3, 6.42% CaO, 4.8% Na_2O, 3.4% MgO, 2.06% K_2O and a small proportion of other compounds.

Brazil Sample MTS-1. This sample is composed of three lithologies (Fig. 1J) Meta-sandstone (90%), andesite (7%) and mica-schist (3%). Meta-sandstone has fine grain size and granular texture. The minerals observed in the thin section were quartz 55%, illite 30%, biotite 12% and opaque minerals 3%. The second is andesite with hypocrystalline, inequigranular porphyritic, medium grain and panidiomorphic texture. Under the microscope anorthite 50%, hornblende 15%, opaque mineral 5% and volcanic glass 30% can be observed. There is a presence of zonation in plagioclase. The last aggregate corresponds to mica-schist has a lepidoblastic texture with fine grain. It presents a banded texture and crenulations. Under the microscope, it is observed: biotite 70%, quartz 25% and opaque minerals 5% (Fig. 2J). The mineralogy obtained with XRD analysis corresponds with quartz, muscovite and chlorite (Table 2). The chemistry obtained with XRF is shown in the Table 3, resulting in a value of 61.02% SiO_2, 18.7% Al_2O_3, 7.51% Fe_2O_3, 5.55% K_2O, 1.8% MgO, 1.36% TiO_2 and a small proportion of other compounds.

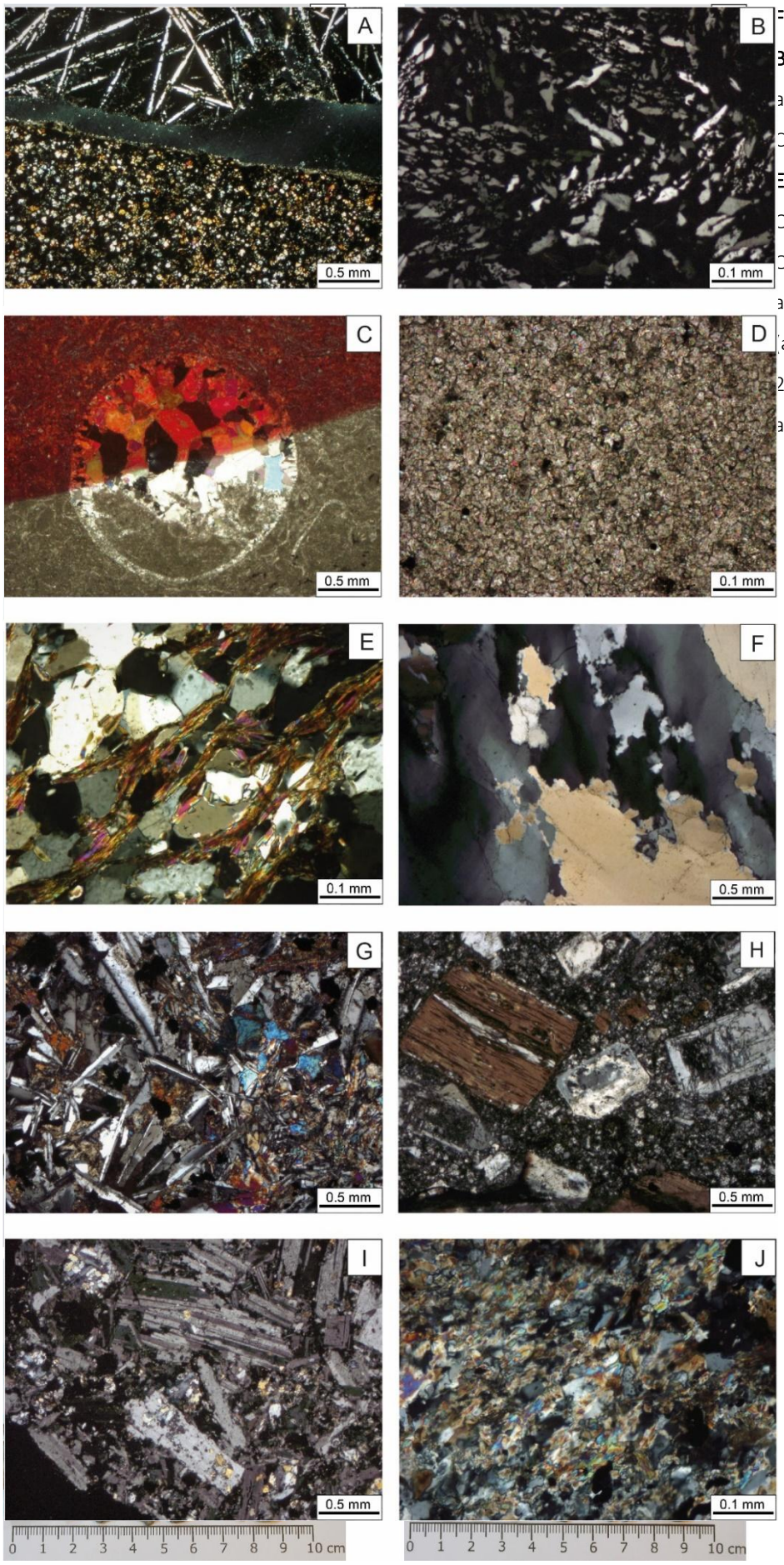

Fig 1. Lithologies studied. **A-B)** Images of thin sections (crossed nicols) of samples: **A-B)** blast furnace slag BFS-1 and BFS-2, **C)** limestone CAL-1, **D)** dolostone DOL-1, **E)** quartzite river gravel QRT-1, **F)** crushed quartzite QRT-2, **G)** ophite OPH-1, **H)** andesite AND-1, **I)** Chile (andesite and others) AND-2, **J)** Brazil (meta-sandstone and others) MTS-1.

3.2. Analysis of microwave heating

Different heating temperatures have been observed when samples are exposed to microwaves (Table 4) includes maximum, minimum, average values and the standard deviation. The average values have been plotted in Figure 3.

Table 4 Average and standard deviationvalues of the thermal data (°C) obtained in the microwave heating test for 200g samples.

	Time [s]																
Sample	0	20	40	60	80	100	120	140	160	180	200	220	240	260	280	300	**Value**
BFS-1	22.5	75.3	126.6	145.5													Avg
	2.5	12.8	17.7	15.7													σ
BFS-2	22.2	110.9	195.2														Avg
	2.7	18.4	32.5														σ
CAL-1	22.3	28.3	31.4	34.5	37.2	38.5	40.6	43.1	45.4	47.8	49.4	51.8	54	56.2	58.2	60.3	Avg
	2.4	3.4	3.9	9.4	4.6	4.7	5.0	5.4	6.0	6.4	6.9	7.2	7.6	7.9	8.5	9.1	σ
DOL-1	22	35.2	43.5	53.7	61.3	68.5	76.3	86.3	92.8	99.6	105.5	112.5	111.8	113.0	117.5	117.3	Avg
	2.4	3.6	3.8	6.0	6.4	7.1	7.4	10.4	10.3	9.9	9.9	11.5	8.9	7.0	7.1	7.0	σ
QRT-1	22.2	29.5	32.5	36.1	39.1	41.7	45.8	48.2	51.2	54.7	58	60.5	63.7	65.1	68.7	69.6	Avg
	2.4	3.4	2.5	2.5	3.2	3.7	4.5	5.9	5.7	6.8	8.0	8.8	9.8	9.4	10.2	10.9	σ
QRT-2	22.0	26.8	29.1	32.4	32.7	33.8	35.4	35.8	37.1	38.3	39.2	40.1	41.0	42.0	42.8	43.7	Avg
	2.5	3.7	4.0	4.1	4.0	4.4	4.1	3.9	3.5	3.4	3.0	3.1	2.7	2.8	2.7	2.5	σ
OPH-1	22.3	43.5	63.4	83.6	97.5	112.6	122.1										Avg
	2.5	4.3	7.5	10.6	11.3	11.4	8.7										σ
AND-1	22.2	42.3	68.0	88.6	108.9	111.4											Avg
	2.4	4.1	7.0	8.3	10.2	8.8											σ
AND-2	22.2	50.5	77.9	104.9	120.9	128.1											Avg
	2.6	7.2	11.8	15.0	15.1	10.6											σ
MTS-1	22.2	36	50.1	64	75.1	87.7	102.3	111.9	121.3	123.1	132.1						Avg
	2.8	3.3	5.1	6.9	7.4	9.1	10.1	8.7	6.6	5.0	2.1						σ

Blast-furnace slag (BFS) BFS-1, exhibits very short heating times. The heating is linear until 40 seconds, hereafter the heating rate decreases, even so, it reaches average temperatures above 145° C in less than 60 seconds. The temperature variability is high, with standard deviations ranging from 12.8 to 17.7.

Blast-furnace slag (BFS) BFS-2. The results obtained are similar to the previous sample but, in this case, heating is linear throughout the entire test. It presents short heating times with average temperatures above 195 °C, in less than 40 seconds. Temperature variability for each time-span is high, with standard deviations ranging from 18.5 to 32.5.

Limestone CAL-1, exhibits very long heating times, with temperatures of only 60 ^{o}C after heating for 300 seconds. During this procedure, the heating is linear, in addition, it is worth noting that the variability of temperatures is low, with standard deviations ranging from 3 to 9.

Dolostone DOL-1, exhibits medium heating times. The heating rate is linear up to 140 seconds when it reaches an average temperature of 86 ^{o}C. Subsequently, the heating rate decreases, reaching an average temperature of around 115 ^{o}C after 300 seconds., the variability of the data is medium, with standard deviations ranging from 3 to 11.

Quartzite river-gravel QRT-1: the results obtained are very similar to sample CAL-1, corresponding to limestone. It shows very long heating times, after heating for 300 seconds average temperatures of 70ºC are not exceeded. During this procedure, heating is linear. In addition, it is worth noting that in the variability of temperatures for a given time is medium, with standard deviations ranging from 2 to 11.

Quartzite QRT-2: the results obtained are very similar to the previous sample, with very long heating times: After heating for 300 seconds, average temperatures do not exceed 45 ^{o}C. During this process, the heating is linear. In addition, the variability of temperatures for a given time is low, with standard deviations ranging from 2.5 to 4.4.

Ophite OPH-1 exhibits short heating times. The heating is linear until 60 seconds, from then on, the heating rate slightly decreases, reaching 122 ^{o}C after 120 seconds of heating. Variability of temperatures for a given time is medium, with standard deviations ranging from 4 to 11.

Andesite AND-1 exhibits short heating times. The heating is linear throughout the entire test. It presents short heating times with average temperatures above 120 ^{o}C after 100 seconds of heating. The variability of temperatures for a given time is medium, with standard deviations ranging from 4.1 to 10.2.

Chile Sample AND-2: the obtained results are similar to the previous sample with a short heating period. The heating rate is linear until 60 seconds and from then onward there is a progressive reduction. The average temperature reached is close to 130 ^{o}C in

100 seconds. The range of variability of temperatures is high with standard deviations ranging from 7 to 14.

Brazil Sample MTS-1: this sample exhibits medium heating times. The rate of heating is constant throughout the test, the average temperature reached is 130 ^{o}C after 200 seconds, in addition, the variability of the data collected is medium with standard deviations ranging from 3 to 10.

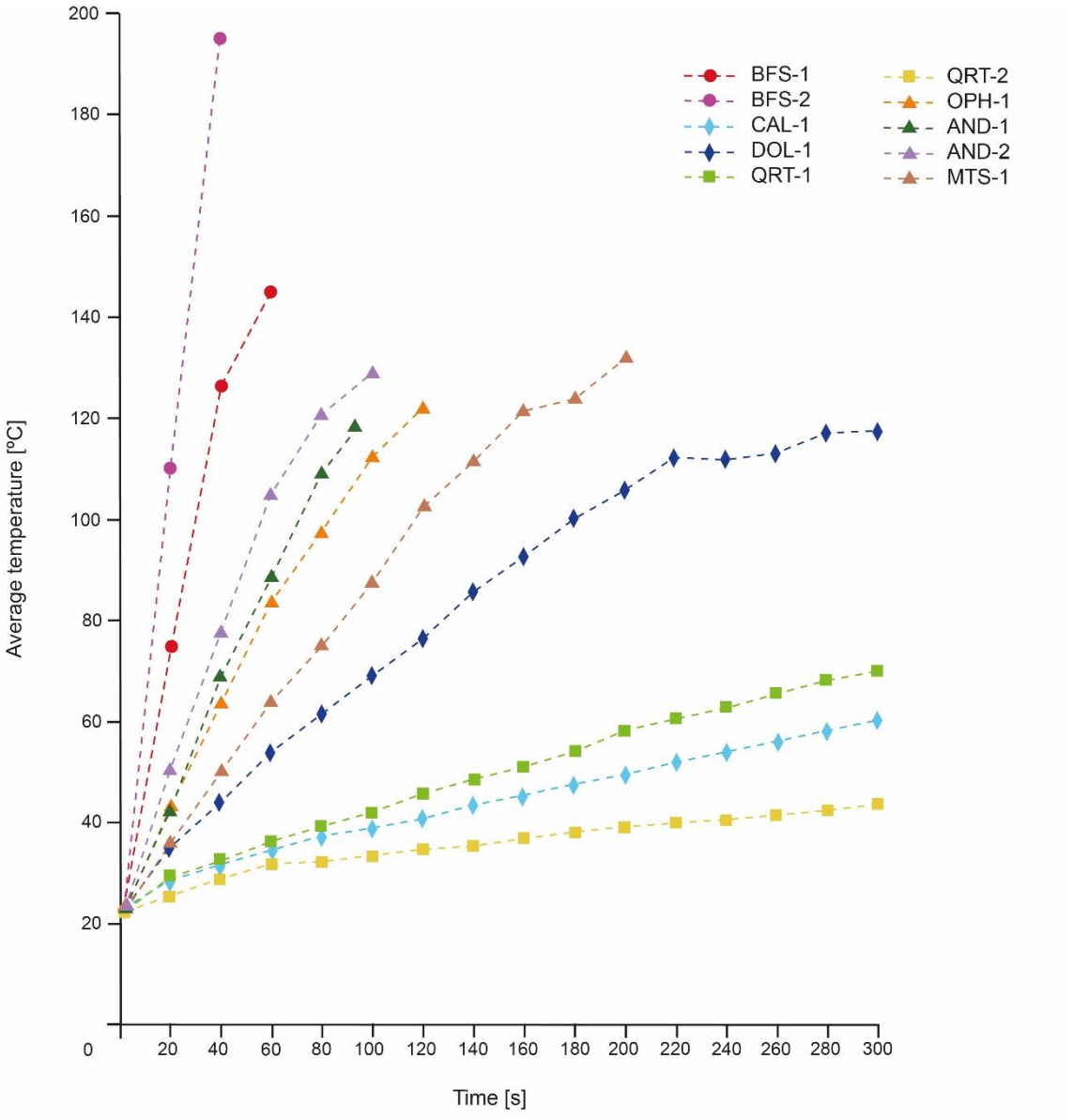

Fig. 3. Evolution of the temperature of the different samples with time. Circles: steelmaking waste; Diamonds: calcareous sedimentary rocks; Squares: metamorphic quartzite rocks, and Triangles: Igneous rocks and mixture of igneous and metamorphic rocks.

As previously mentioned in the methodology section, during the warm-up, energy consumption was measured, and Figure 4 shows the consumption of the process (Wh/kg) versus the surface temperature of the sample (^{o}C). These consumption measurements were taken every 20 s. Subsequently, the data were approximated by a linear curve where the correlation coefficients were close to 1. In this graph, it is possible to see that different aggregates give rise to different consumption ratios.

The slope of the estimated regression line represents the susceptibility of the aggregate to be heated by microwave radiation (ΔT/Energy consumption/kg). The higher the slope, the better the susceptibility to microwave and the energy efficiency of the heating process. Figure 5 shows the susceptibility to microwave heating of the aggregates under study. Samples show different susceptibilities, from very high (BFS-1 and BFS-2), high (OPH-1, AND-1 and AND-2), intermediate (DOL-1 and MTS-1); to very low (CAL-1, QRT-1, and QRT-2).

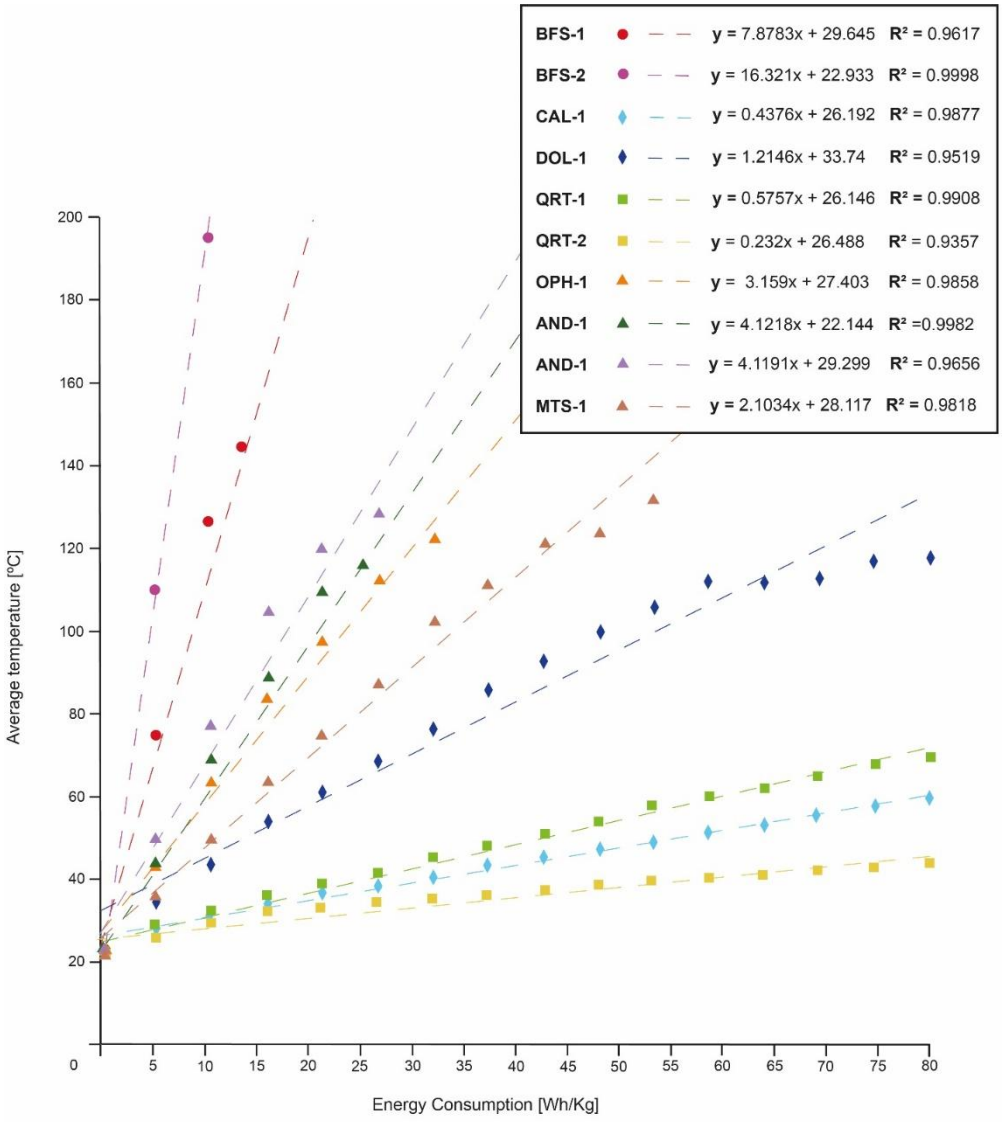

Fig. 4. Energy consumed versus temperature reached by the aggregates. Circles: steelmaking waste; Diamonds: calcareous sedimentary rocks; Squares: metamorphic quartzite rocks, and Triangles: Igneous rocks and mixture of igneous and metamorphic rocks.

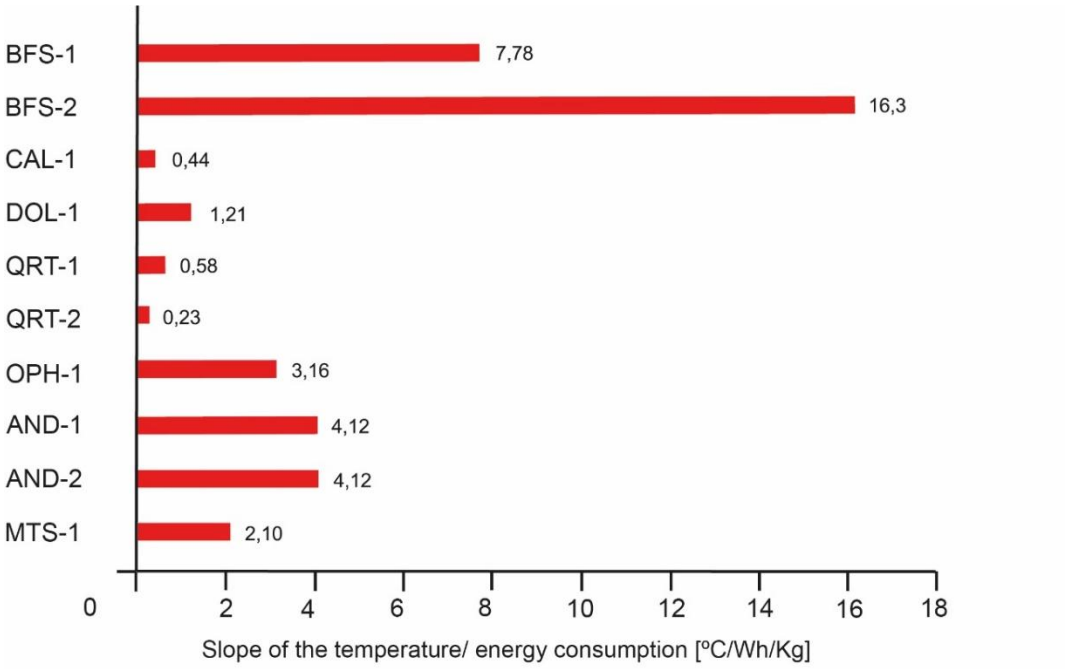

Fig. 5. Slope of the temperature versus energy consumption. (Susceptibility to microwaves).

4. Discussion

Microwave susceptibility presents a wide range of variation within the samples under study; some heating very quickly (blast-furnace slags BFS-1 and BFS-2), quickly (ophite OPH-1 and andesites AND-1 and AND-2), intermediate heating rates (dolostone DOL-1 and meta-sandstone MTS-1), and others heating very slowly (limestone CAL-1, quartzite river-gravel QRT-1 and quartzite QRT-2).

4.1. Classification according to susceptibility to microwave radiation

In accordance with the susceptibility to microwave heating, the samples under study have been classified into four categories.

Very Quick Heating Samples

They have a very high susceptibility to microwaves; this group is composed of BFS (BFS-1 and BFS-2). The origin of both samples is similar, they were formed by the cooling of metal residues, so they have been classified in the same genetic group. They

are formed by a vitreous phase and a mineral phase of melilite that presents variable morphologies. Both samples have high concentrations of CaO, Fe_2O_3, Al2O_3, MgO and Cr_2O_3. The sample BFS-2 shows higher average temperatures although the minimum temperatures are very similar in both samples. Variability of the measurements is high in both samples but slightly higher in BFS-2.

Quick Heating Samples

They have a high susceptibility to microwaves; this group is composed of two andesites (AND-1 and AND-2) and one ophite sample (OPH-1). The rocks in this group are volcanic or sub-volcanic, so they have similar characteristics, such as crystal size or ferromagnesian minerals content, approximately 25%. The difference between the rocks is the composition of the main ferromagnesian mineral, in the andesites it is hornblende while in the ophite it is augite. In addition, they have high concentrations of SiO_2, Fe_2O_3, Al_2O_3, MgO and in the ophite also CaO. The rocks heat quick, and both andesite samples (AND-1 and AND-2) behave similarly. In contrast, ophite has a slower heating rate, needing in average 20 seconds more than andesites to reach the same temperature. The range of variability of the measurements is similar in these two lithologies.

Medium Heating Samples

They have an intermediate susceptibility to microwaves. This group is composed of dolostone (DOL-1) and meta-sandstone samples (MTS-1). Compositionally they are very different, since dolostone is a calcareous sedimentary rock, and the meta-sandstone is a siliciclastic sedimentary rock with a high percentage of quartz, which went through a process of metamorphism. In terms of their chemistry, these two samples are very different: dolostone is rich in CO_2, CaO and MgO and meta-sandstone in SiO_2, Al_2O_3 and Fe_2O_3. The heating rate is intermediate, although it is slightly faster in the meta-sandstone (dolostone needs between 30-40 seconds more to reach the same temperature), even though the variability of the measurements in both samples is similar.

Very Low Heating Samples

The group of samples with a low susceptibility to microwaves is composed of the limestone (CAL-1), the quartzite river-gravel (QRT-1), and the crushed quartzite (QRT-2) samples. Quartzites are compositionally different from limestone, since quartzites are formed mainly by quartz and have a metamorphic origin, while limestone is a sedimentary carbonate rock. Quartzites, have high percentages of SiO_2 while limestone has high percentages of CO_2 and CaO, so they do not share oxides in high concentrations in their composition. Heating of the samples is slow, slightly quicker in the case of the limestone sample (DOL-1) and in the quartzite river-gravel sample (QRT-1). The sample corresponding to crushed quartzite presents the slowest heating of all studied samples. It would be reasonable for the quartzite river-gravel (QRT-1) to follow a similar heating pattern, since it is mainly formed by quartz. However, the presence in the sample of some carbonatic pebbles increases its average heating rate.

4.2. Optimal heating temperature: T70 parameter

After carrying out the tests and determining the differential heating potential among the different types of aggregates, a quantitative classification will be established. In this sense, it will be possible to know which aggregates present the best characteristics to be used in road pavements to be assisted with microwaves for healing. Combining the information of the studies [7,9,13,14], an optimal temperature of 70 ^{o}C was chosen as the heating target for the aggregates.

The T70 parameter is the time (seconds) that a 200g sample of aggregate requires to reach 70 ^{o}C from an ambient temperature of 20 ^{o}C by a microwave radiation, with an output power of 700W and a frequency of 2.45 Gz. In this way, knowing the time required to reach the optimum heating temperature by radiation with a fixed microwave power, the aggregates could be classified according to their adequacy for use in asphalt mixtures.

Table 5 shows the values obtained from the samples under study, their T70 parameter values, and the regression equation that crosses the target temperature of 70 ^{o}C for each lithology. For those samples not reaching a temperature of 70 ^{o}C, extrapolation has been carried out to estimate the time required for the sample to reach target temperature.

Five classes have been proposed according to the T70 parameter (Fig. 6). Time length of the classes increases progressively since it is more relevant to separate more precisely, samples that have quicker heating. The first class corresponds with the samples with very quick heating: 70 ^{o}C in less than 30 seconds. The second class includes the samples that require between 30 and 60 seconds to reach 70 ^{o}C. In the third class, the samples showed medium heating, reaching 70 ^{o}C in 120 seconds. Samples in the fourth class (slow heating) need between 120 and 240 seconds to reach 70 ^{o}C. Finally, the fifth-class includes the samples that, due to the very slow heating, require more than 240 seconds to reach the target temperature.

Table 5 Heating times to reach 70 ºC, regression equation and value of R^2 for each sample. Data extracted from Figure 3.

Sample	T70	Formula
BFS-1	19	y = 2,.1015x + 29.43 **R²** = 0.9635
BFS-2	11	y = 4.325x + 22.933 **R²** = 0.9998
CAL-1	376	y =0.1167x + 26.177 **R²** = 0.9878
DOL-1	112	y = 0.324x + 33.698 **R²** = 0,952
QRT-1	286	y = 0,1536x + 26,126 **R²** = 0.9908
QRT-2	703	y = 0.0619x + 26.48 **R²** = 0.9358
OPH-1	51	y = 0.8423x + 27.318 **R²** = 0.986
AND-1	44	y = 1.0985x + 22.06 **R²** = 0.9982
AND-2	37	y = 1.0967x + 29.248 **R²** = 0.9653
MTS-1	75	y = 0.5611x + 28.05 **R²** = 0.9817

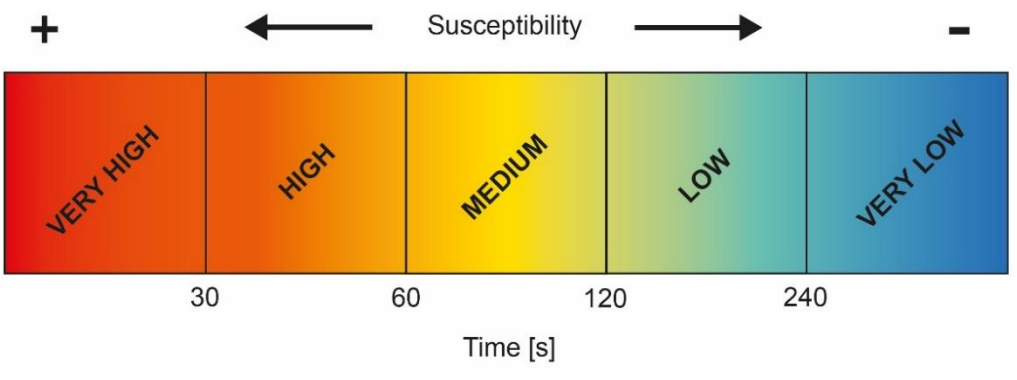

Fig. 6. Classes proposed for the T70 parameter.

It is also necessary to consider economic, environmental and geological factors for the aggregates selection. For instance, the scarcity of a certain type of rock in a country is a constraining factor. The use of a rock that has short heating times, but that is not abundant in a country would result in high economic and environmental costs due to higher transportation distances.

Samples with very high susceptibility to microwaves (VHS), determined by a T70 value less than 30 seconds are BFS (BFS-1 and BFS-2). Gallego *et al.* [27] also studied this type of aggregate as a component of asphalt mixtures, concluding that, in spite of the good heating times, it should be only used as an additive (up to 5%) to facilitate the heating of a mixture containing other less susceptible aggregates.

The samples with high susceptibility to microwaves (HS), a T70 between 30 and 60 s, are both andesites (AND-1 and AND-2) and the ophite (OPH-1) rocks. The main limiting factor for the employment of these types of aggregates for microwave assisted-healing is their geographical distribution. Areas rich in andesite in the world are far apart from each other and this has an impact on their composition. This was carried out by testing the impact of the different location and composition in the behaviour samples from Spain (AND-1) and Chile (AND-2).[51]. In Spain at present, only one quarry extracts andesite [36], which means transport distances are very long. Therefore, its use would only be interesting in areas with an abundance of this type of rock resulting in short transport distances. The ophite sample presents a T70 of 50 seconds, and in Spain several deposits of this rock can be found. More than 1 million tons of ophite are

extracted every year in Spain from several quarries. [36]. Therefore, this rock is used in Spain, since it has good heating times and a wide geographical distribution.

Samples in the **T70 class between 60 and 120 seconds** (medium susceptibility, MS), are the dolomite rock (DOL-1) and the meta-sandstone (MTS-1). Meta-sandstone presents heating times of 75 seconds, so it could be considered acceptable from point of view of heating. The Dolostone sample has a heating time of approximately 110 seconds to reach 70 ^{o}C. Dolostone is common in Spain and in other countries. In Spain approximately 6 million tons are extracted per year [36]. This type of rock is usually formed in diagenetic stages, and y have better characteristics in terms of wearing [52]. The abundance and good mechanical characteristics make dolostone suitable to be used in Spain, although heating times are higher than other lithologies.

Finally, the group of rocks that have a very low susceptibility (VLS) to microwaves **(T70 >240 s)** are the quartzite river-gravel, the crushed quartzite, and the limestone. These samples needed more than 280 seconds to reach a temperature of 70 ^{o}C, which implies high energy and time costs. Although they are abundant in Spain; more than 100 million tons are extracted per year [36], their slow heating rate makes this type of rock of little interest for the microwave assisted-healing process.

The heating results and their classification according to parameter T70 are shown in Table 6. The use of the T70 parameter proposed in this work will help to choose the lithologies that present better heating behaviour for the technique of healing by microwaves.

Table 6 Classification of the samples studied with respect to the parameter T70.

Sample	T70 Class	Recommendation
BFS-1	Very high	Good (additive)
BFS-2	Very high	Good (additive)
CAL-1	Very low	Excluded
DOL-1	Medium	Acceptable
QRT-1	Very low	Excluded
QRT-2	Very low	Excluded
OPH-1	High	Good
AND-1	High	Good (probable transport limitation)
AND-2	High	Good
MTS-1	Medium	Acceptable

As it has been demonstrated, there is a differential heating between samples. This has been revealed by other authors, where they analyse the heating of aggregates

with very different compositions [25,37]. After a bibliographic review, they propose different causes of differential heating, including: a) dielectric values of minerals or rocks [25,37,53], b) iron content [14,27], c) mineralogical and chemical composition [53–55], d) size of the crystals that form minerals [56,57]. However, no consensus has been reached and therefore further work is required to elucidate the precise causes of differential heating of different types of rocks.

5. Conclusions

The results of this study show that the application of microwaves produces a differential heating response among the aggregates studied. The use in asphalt mixtures of aggregates prone to heating under microwaves would facilitate the assisted healing treatments with microwaves.

An assay procedure has been developed and an indicator proposed to classify the aggregates according to their suitability for assisted healing treatments by microwave radiation. The proposed parameter is the time required to reach 70 °C beginning at 20 °C (laboratory temperature) following the assay protocol, by a microwave radiation, with an output power of 700W and a frequency of 2.45 Gz. Five classes have been defined according to the susceptibility of aggregates to microwaves. The aggregates with a higher heating susceptibility are more suitable for microwave assisted-healing treatments.

The samples analysed to test the procedure gave the following results: (VHS) very high susceptibility: blast furnace slag (BFS); (HS) high susceptibility: andesite and ophite; (MS) medium susceptibility: dolostone and meta-sandstone; (LS) low susceptibility: none of the 10 samples analysed belong to this class; and (VLS) very low susceptibility: quartzite and limestone.

The results of this study could be used to optimise the composition of asphalt mixtures suitable for microwave assisted-healing treatments. These results could also serve to predict the energy efficiency of the healing treatment in existing roads,

incorporating, among other variables, the composition of the aggregates employed during their construction.

Acknowledgments

We would like to thank Ofitas de San Felices, Maquinaria Arbolea, and Benito Arnó e Hijos for providing samples for this study and CAI of Geological Techniques of the Complutense University of Madrid for their analyses. Special thanks to the Editor and Reviewers for their comments and suggestions that have led to improvements in the manuscript. This study was financed by the research project BIA 2017-86253-C2-1-R of the Ministerio de Economía y Empresa of Spain.

References

[1] M. Ameri, S. Hesami, H. Goli, Laboratory evaluation of warm mix asphalt mixtures containing electric arc furnace (EAF) steel slag, Constr. Build. Mater. 49 (2013) 611-617. doi:10.1016/j.conbuildmat.2013.08.034.

[2] P. Bazin, J.B. Saunier, Deformability, fatigue and healing properties of asphalt mixes, en: Proc. Second Int. Conf. Struct. Des. Asph. Pavements, 1967: pp. 553-569.

[3] A. Menozzi, A. Garcia, M. N.Partl, G. Tebaldi, P. Schuetz, Induction healing of fatigue damage in asphalt test samples, Constr. Build. Mater. 74 (2015) 162-168. doi:10.1016/j.conbuildmat.2014.10.034.

[4] P. Ayar, F. Moreno-navarro, M.C. Rubio-g, The healing capability of asphalt pavements : a state of the art review, 113 (2016) 28-40. doi:10.1016/j.jclepro.2015.12.034.

[5] M.C. Phillips, Multi-step models for fatigue and healing, and binder properties involved in healing, en: Eurobitume Work. Perform. Relat. Prop. Bitum. Bind. Luxemb., 1998.

[6] J. Gallego, M.A. Del Val, V. Contreras, A. Páez, Heating asphalt mixtures with microwaves to promote self-healing, Constr. Build. Mater. 42 (2013) 1-4. doi:10.1016/j.conbuildmat.2012.12.007.

[7] A. García, E. Schlangen, M. Van De Ven, D. Van Vliet, Crack repair of asphalt concrete with induction energy, Heron. 56 (2011) 37-48.

[8] Á. García, E. Schlangen, M. Van De Ven, Q. Liu, A simple model to define induction heating in asphalt mastic, Constr. Build. Mater. 31 (2012) 38-46. doi:10.1016/j.conbuildmat.2011.12.046.

[9] Á. García, Self-healing of open cracks in asphalt mastic, Fuel. 93 (2012) 264-272. doi:10.1016/j.fuel.2011.09.009.

[10] Q. Liu, W. Yu, S. Wu, E. Schlangen, P. Pan, A comparative study of the induction healing behaviors of hot and warm mix asphalt, Constr. Build. Mater. 144 (2017) 663-670. doi:10.1016/j.conbuildmat.2017.03.195.

[11] D.N. Little, A. Bhasin, Exploring Mechanism of H ealing in Asphalt Mixtures and Quantifying its Impact, en: Self Heal. Mater., 2007: pp. 205-218. doi:10.1007/978-1-4020-6250-6_10.

[12] S. Singh, D. Gupta, V. Jain, A.K. Sharma, Microwave processing of materials and applications in manufacturing industries: A Review, Mater. Manuf. Process. 30 (2015) 1-29. doi:10.1080/10426914.2014.952028.

[13] Q. Liu, E. Schlangen, M. Van De Ven, G. Van Bochove, J. Van Montfort, Evaluation of the induction healing effect of porous asphalt concrete through four point bending fatigue test, Constr. Build. Mater. 29 (2012) 403-409. doi:10.1016/j.conbuildmat.2011.10.058.

[14] X. Zhu, Y. Cai, S. Zhong, J. Zhu, H. Zhao, Self-healing efficiency of ferrite-filled asphalt mixture after microwave irradiation, Constr. Build. Mater. 141 (2017) 12-22. doi:10.1016/j.conbuildmat.2017.02.145.

[15] J. Norambuena-Contreras, A. Garcia, Self-healing of asphalt mixture by microwave and induction heating, Mater. Des. 106 (2016) 404-414. doi:10.1016/j.matdes.2016.05.095.

[16] B. Gómez-Meijide, H. Ajam, A. Garcia, S. Vansteenkiste, Effect of bitumen properties in the induction healing capacity of asphalt mixes, Constr. Build. Mater. 190 (2018) 131-139. doi:10.1016/j.conbuildmat.2018.09.102.

[17] G. Flores, J. Gallego, F. Giuliani, F. Autelitano, Aging of asphalt binder in hot pavement rehabilitation, Constr. Build. Mater. 187 (2018) 214-219. doi:10.1016/j.conbuildmat.2018.07.216.

[18] J.S. Daniel, Y.R. Kim, Laboratory evaluation of fatigue damage and healing of asphalt mixtures, J. Mater. 13 (2001) 434-440. doi:10.1061/(ASCE)0899-1561(2001)13:6(434).

[19] R. Mitchell, D. Woodward, D. Ryan, Use of Microwave Conditioning to Rapidly Age Asphalt Mixes, en: Airf. Highw. Pavement 2013 Sustain. Effic. Pavements, 2013: pp. 1211-1218. doi:10.1061/9780784413005.102.

[20] T.M. Phan, D.-W. Park, T.H.M. Le, Crack healing performance of hot mix asphalt containing steel slag by microwaves heating, Constr. Build. Mater. 180 (2018) 503-511. doi:10.1016/j.conbuildmat.2018.05.278.

[21] J. Norambuena-Contreras, A. Gonzalez, J.L. Concha, I. Gonzalez-Torre, E. Schlangen, Effect of metallic waste addition on the electrical, thermophysical and microwave crack-healing properties of asphalt mixtures, Constr. Build. Mater. 187 (2018) 1039-1050. doi:doi.org/10.1016/j.conbuildmat.2018.08.053.

[22] J.Á. Menéndez, Á.H. Moreno, Aplicaciones industriales del calentamiento con energía microondas, 2017.

[23] I.N. Levine, Físico-Química, en: Físico-Química, 4ª Edición, McGraw-Hill, Madrid, 1993.

[24] J.M.R. Bélanger, J.R.J. Paré, O. Poon, C. Fairbridge, S. Ng, S. Mutyala, R. Hawkins, Remarks on Various Applications of Microwave Energy, J. Microw. Power Electromagn. Energy. 42 (2016) 24-44. doi:10.1080/08327823.2007.11688597.

[25] A. Benedetto, A. Calvi, A pilot study on microwave heating for production and recycling of road pavement materials, Constr. Build. Mater. 44 (2013) 351-359. doi:10.1016/j.conbuildmat.2013.02.082.

[26] J. Prado-Gonjal, Síntesis- asistida por microondas- y caracterización de materiales inorgánicos, Universidad Complutense de Madrid, 2014. doi:10.1016/0021-9517(90)90216-7.

[27] J. Gallego, M.A. Del Val, V. Contreras, A. Páez, Use of additives to improve the capacity of bituminous mixtures to be heated by means of microwaves, Mater. Construcción. 67 (2017) 110. doi:10.3989/mc.2017.00416.

[28] A. García, J. Norambuena-Contreras, M.N. Partl, A parametric study on the influence of steel wool fibers in dense asphalt concrete, Mater. Struct. 47 (2014) 1559-1571. doi:10.1617/s11527-013-0135-0.

[29] A. González, J. Valderrama, J. Norambuena-Contreras, Microwave crack healing on conventional and modified asphalt mixtures with different additives: an experimental approach, Road Mater. Pavement Des. 20 (2019) 149-162. doi:10.1080/14680629.2019.1587493.

[30] M.M. Karimi, M.K. Darabi, H. Jahanbakhsh, B. Jahangiri, J.F. Rushing, Effect of steel wool fibers on mechanical and induction heating response of conductive asphalt concrete, Int. J. Pavement Eng. (2019) 1-14. doi:10.1080/10298436.2019.1567918.

[31] A.P. Pérez Fortes, Calidad y durabilidad de áridos metamórficos empleados en capas de rodadura gallegas bajo el efecto de la sal y una climatología extrema, Facultad de Ciencias Geológicas; Universidad Complutense de Madrid, 2016.

[32] A.P. Pérez Fortes, S. Anastasio, E. Kuznetsova, S.W. Danielsen, Behaviour of crushed rock aggregates used in asphalt surface layer exposed to cold climate conditions, Environ. Earth Sci. 75 (2016) 1414-1424. doi:10.1007/s12665-016-6191-3.

[33] R.G. Bosisio, J. Spooner, J. Grɑnger, Asphalt road maintenance with a mobile microwave power unit, J. Microw. Power. 9 (1974) 381-386.

[34] J. Gao, H. Guo, X. Wang, P. Wang, Y. Wei, Z. Wang, Y. Huang, B. Yang, Microwave deicing for asphalt mixture containing steel wool fi bers Intensity, J. Clean. Prod. 206 (2019) 1110-1122. doi:10.1016/j.jclepro.2018.09.223.

[35] Z. Liu, X. Yang, Y. Wang, S. Luo, Engineering properties and microwave heating induced ice-melting performance of asphalt mixture with activated carbon powder filler, Constr. Build. Mater. 197 (2019) 50-62. doi:10.1016/j.conbuildmat.2018.11.094.

[36] METAD, Estadística Minera de España, 2016.

[37] P. Hartlieb, M. Toifl, F. Kuchar, R. Meisels, T. Antretter, Thermo-physical properties of selected hard rocks and their relation to microwave-assisted comminution, Miner. Eng. 91 (2016) 34-41. doi:10.1016/j.mineng.2015.11.008.

[38] G.D. Airey, A.C. Collop, S.E. Zoorob, R.C. Elliott, The influence of aggregate, filler and bitumen on asphalt mixture moisture damage, Constr. Build. Mater. 22 (2008) 2015-2024. doi:10.1016/j.conbuildmat.2007.07.009.

[39] A. Rezaei, E. Masad, A. Chowdhury, P. Harris, Predicting Asphalt Mixture Skid Resistance by Aggregate Characteristics and Gradation, Transp. Res. Rec. J. Transp. Res. Board. 2104 (2009) 24-33. doi:10.3141/2104-03.

[40] European Committee for Standardization (CEN), Natural stone test methods. Petrographic examination (EN 12407: 2007)

[41] F.H. Chung, Quantitative interpretation of X-ray diffraction patterns of mixtures. III. Simultaneous determination of a set of reference intensities, J. Appl. Crystallogr. 8 (1975) 17-19. doi:10.1107/S0021889875009454.

[42] A. Bonati, S. Rainieri, G. Bochicchio, B. Tessadri, F. Giuliani, Characterization of thermal properties and combustion behaviour of asphalt mixtures in the cone calorimeter, Fire Saf. J. 74 (2015) 25-31. doi:10.1016/j.firesaf.2015.04.003.

[43] European Committee for Standardization (CEN), Natural stone. Terminology. (EN 12670: 2003)

[44] R. Le Maitre, A. Streckeisen, B. Zanettin, M. Le Bas, B. Bonin, P. Bateman, Igneous Rocks: A Classification and Glossary of Terms: Recommendations of the International Union of Geological Sciences Subcommission on the Systematics of Igneous Rocks, 2.ª ed., Cambridge University Press, Cambridge, 2002. doi:DOI: 10.1017/CBO9780511535581.

[45] R.J. Dunham, Classification of Carbonate Rocks According to Depositional Texture1, Classif. Carbonate Rocks—A Symp. 1 (1962) 0. doi:10.1007/978-3-642-68423-4.

[46] G.M. Friedman, Terminology of crystallization textures and fabrics in sedimentary rocks, J. Sediment. Res. 35 (1965) 643-655. doi:10.1306/74D7131B-2B21-11D7-8648000102C1865D.

[47] F.J. Turner, J.J. Verhoogen, Igneous and metamorphic petrology. McGraw-Hill Book Company, New York SE No. 552.2 TUR (1951)

[48] F. Puertas, Escorias de alto horno: composición y comportamiento hidráulico, Mater. Construcción. 43 (1993) 37-48. doi:10.3989/mc.1993.v43.i229.687.

[49] I.A. Oyarzun Kneer, Influencia de las escorias de cobre en la fabricación de hormigón, (Doctoral dissertation) Universidad Austral de Chile, 2013.

[50] M.P. Alaejos, M. Sánchez, F. Sinis, H. Cano, Catálogo de Residuos Utilizables en Construcción, CEDEX para el Minist. Medio Ambient. (2008).

[51] SERNAGEOMIN, 2003. Mapa Geológico de Chile: versión digital. Servicio Nacional de Geología y Minería, Publicación Geológica Digital, No. 4 (CD-ROM, versión1.0, 2003). Santiago. ISSN-0717-9006.

[52] J.T. Tamayo, C.G. Guevara, J.C. Vargas, Estudio de la degradación de los agregados pétreos durante la vida útil de los pavimentos, Ing. e Investig. (1983) 13-21.

[53] G. ming Lu, Y. hui Li, F. Hassani, X. Zhang, The influence of microwave irradiation on thermal properties of main rock-forming minerals, Appl. Therm. Eng. 112 (2017) 1523-1532. doi:10.1016/j.applthermaleng.2016.11.015.

[54] J. Gao, A. Sha, Z. Wang, Z. Tong, Z. Liu, Utilization of steel slag as aggregate in asphalt mixtures for microwave deicing, J. Clean. Prod. 152 (2017) 429-442. doi:10.1016/j.jclepro.2017.03.113.

[55] T. Peinsitt, H. Kargl, U. Restner, N.A. Sifferlinger, Microwave heating of dry and water saturated basalt , granite and sandstone Friedemar Kuchar * Philipp Hartlieb and Peter Moser, en: Int. J. Min. Miner. Eng., 2010: pp. 18-29. doi:10.1504/IJMME.2010.031810.

[56] N. Standish, H. Worner, G. Gupta, Temperature Distribution in Microwave-Heated Iron Ore-Carbon Composites, J. Microw. Power Electromagn. Energy. 25 (2016) 75-80. doi:10.1080/08327823.1990.11688114.

[57] J.B. Salsman, R.L. Williamsont, W.K. Tolley, D.A. Rice, Short-pulse microwave treatment of disseminated sulfide ores, Miner. Eng. 9 (1996) 43-54. doi:10.1016/0892-6875(95)00130-1.

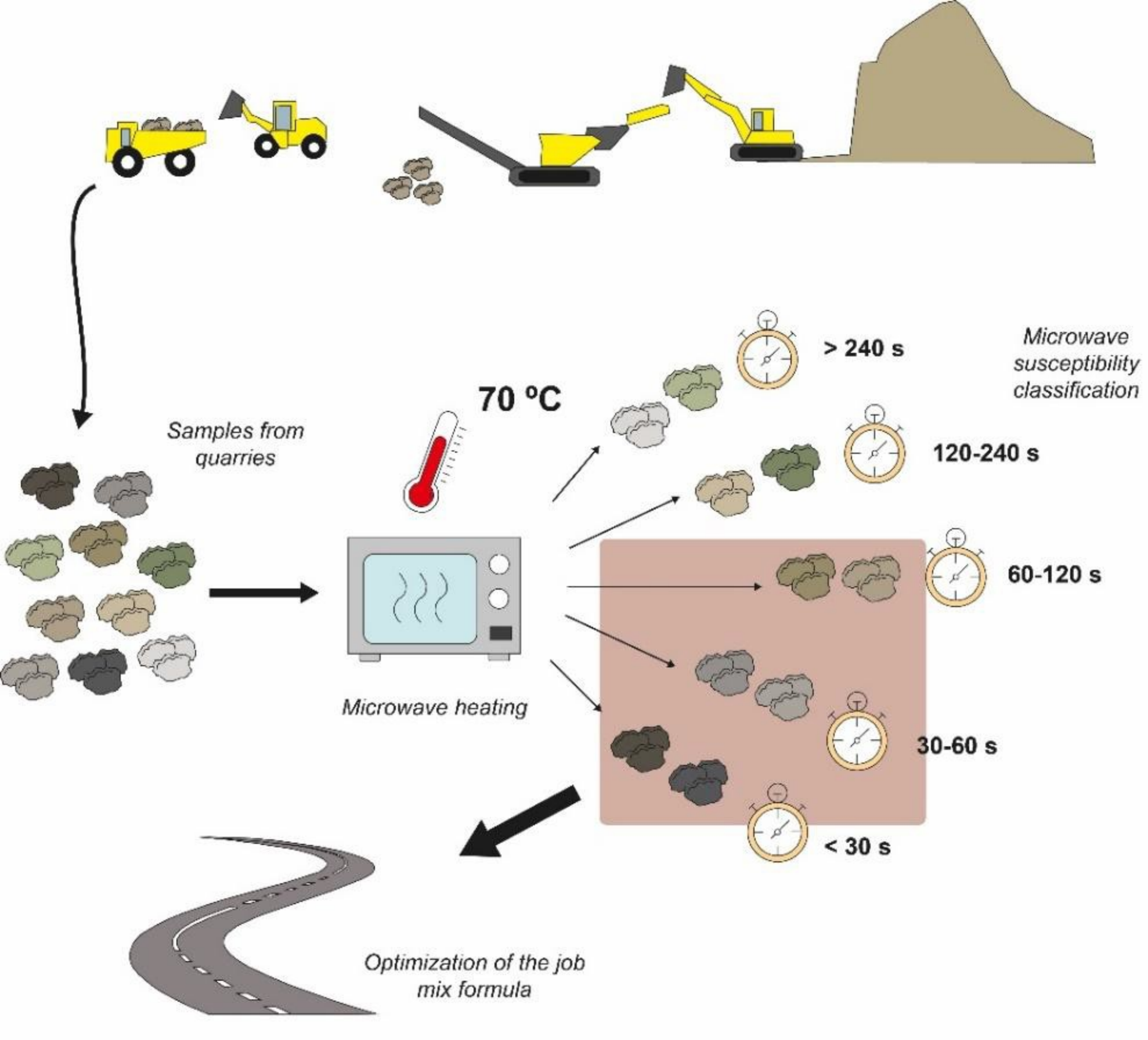
Samples from quarries
70 ºC
Microwave heating
Microwave susceptibility classification
> 240 s
120-240 s
60-120 s
30-60 s
< 30 s
Optimization of the job mix formula


A
0 1 2 3 4 5 6 7 8 9 10 cm


B
0 1 2 3 4 5 6 7 8 9 10 cm


C
0 1 2 3 4 5 6 7 8 9 10 cm


D
0 1 2 3 4 5 6 7 8 9 10 cm


E
0 1 2 3 4 5 6 7 8 9 10 cm


F
0 1 2 3 4 5 6 7 8 9 10 cm


G
0 1 2 3 4 5 6 7 8 9 10 cm


H
0 1 2 3 4 5 6 7 8 9 10 cm


I
0 1 2 3 4 5 6 7 8 9 10 cm


J
0 1 2 3 4 5 6 7 8 9 10 cm

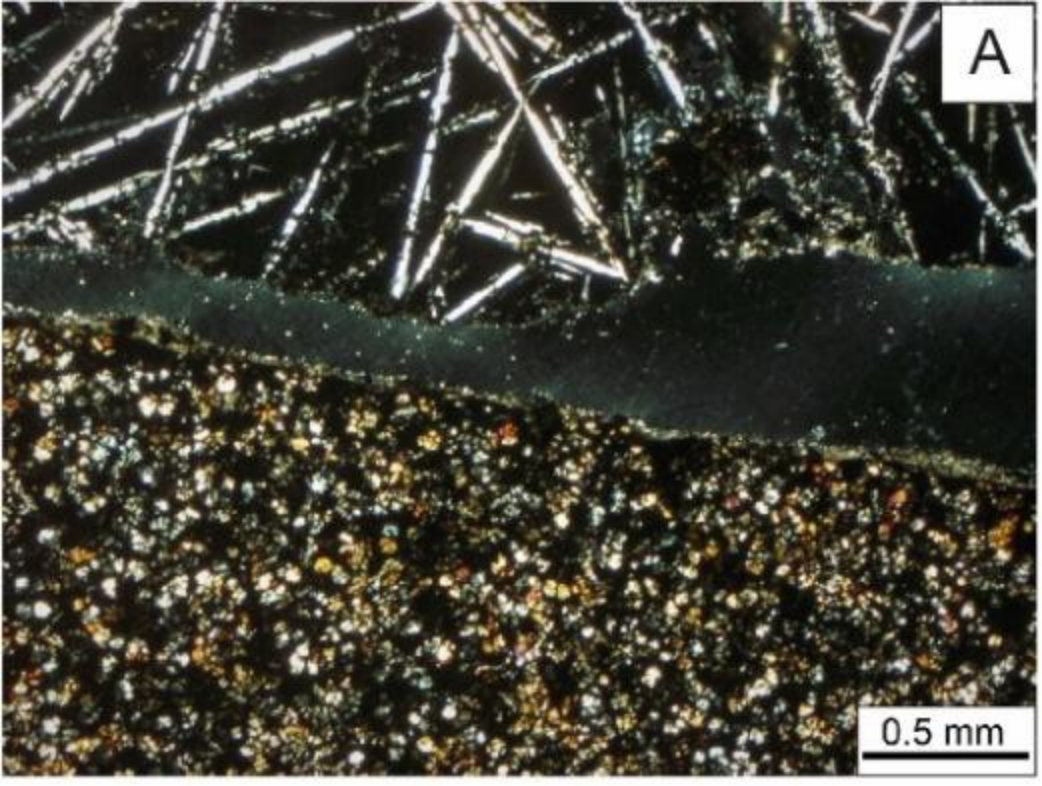
A
0.5 mm

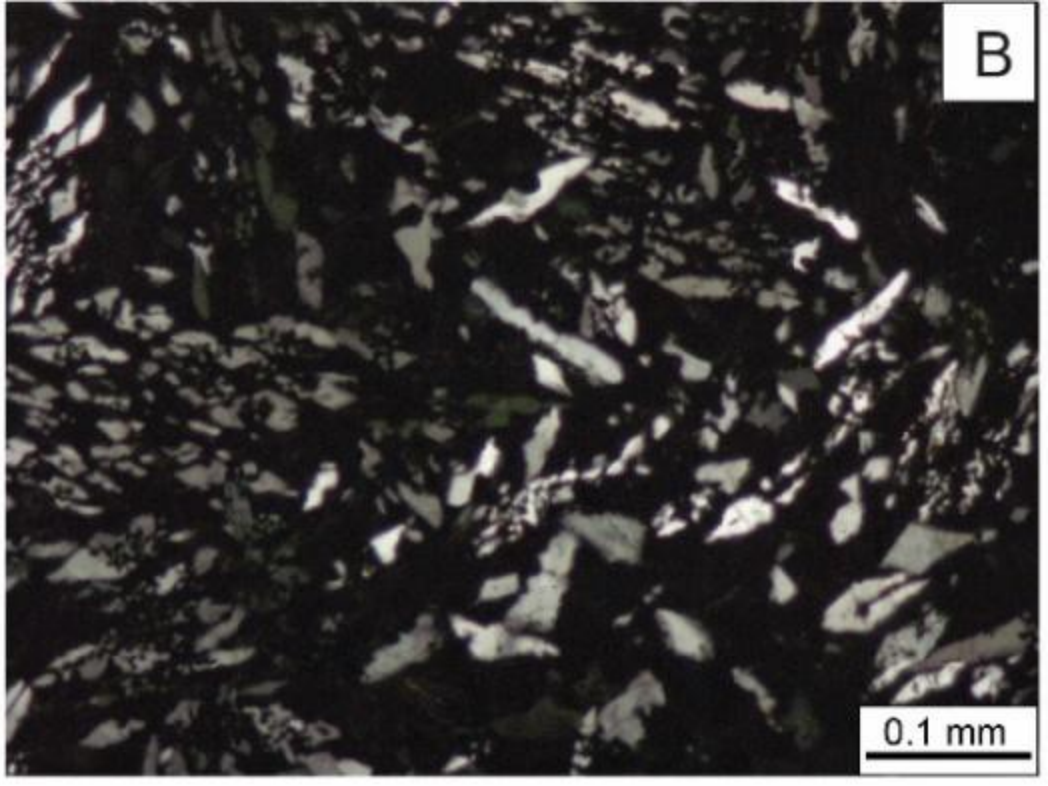
B
0.1 mm

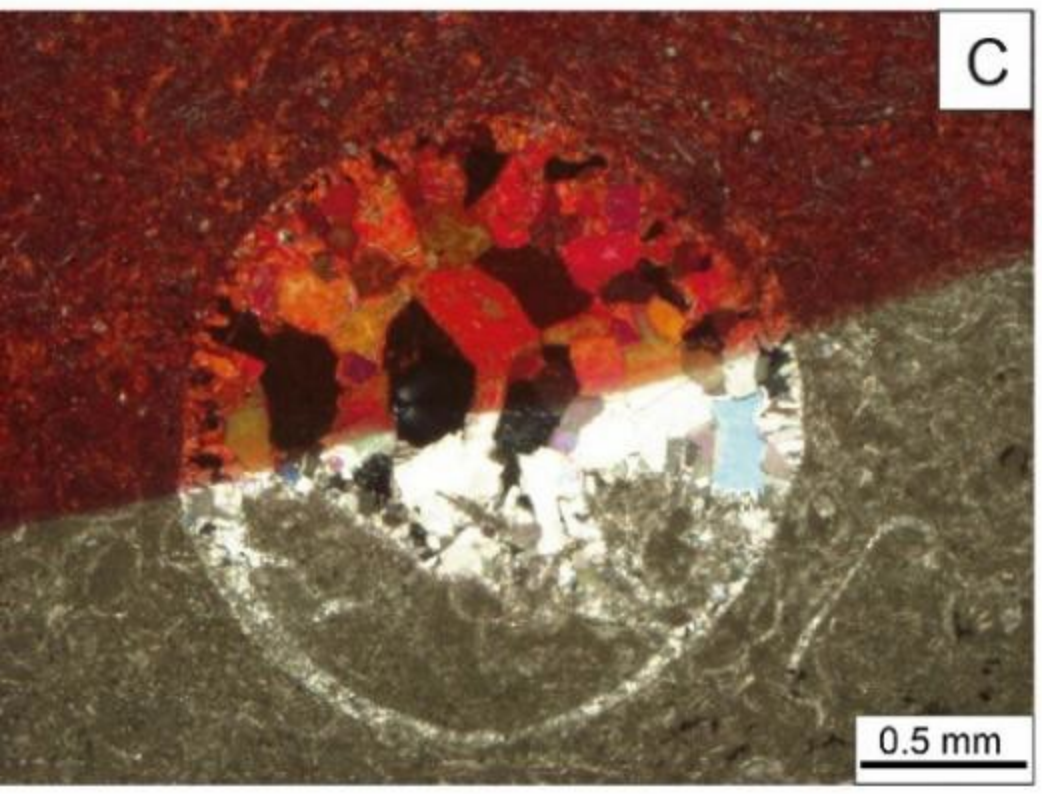
C
0.5 mm

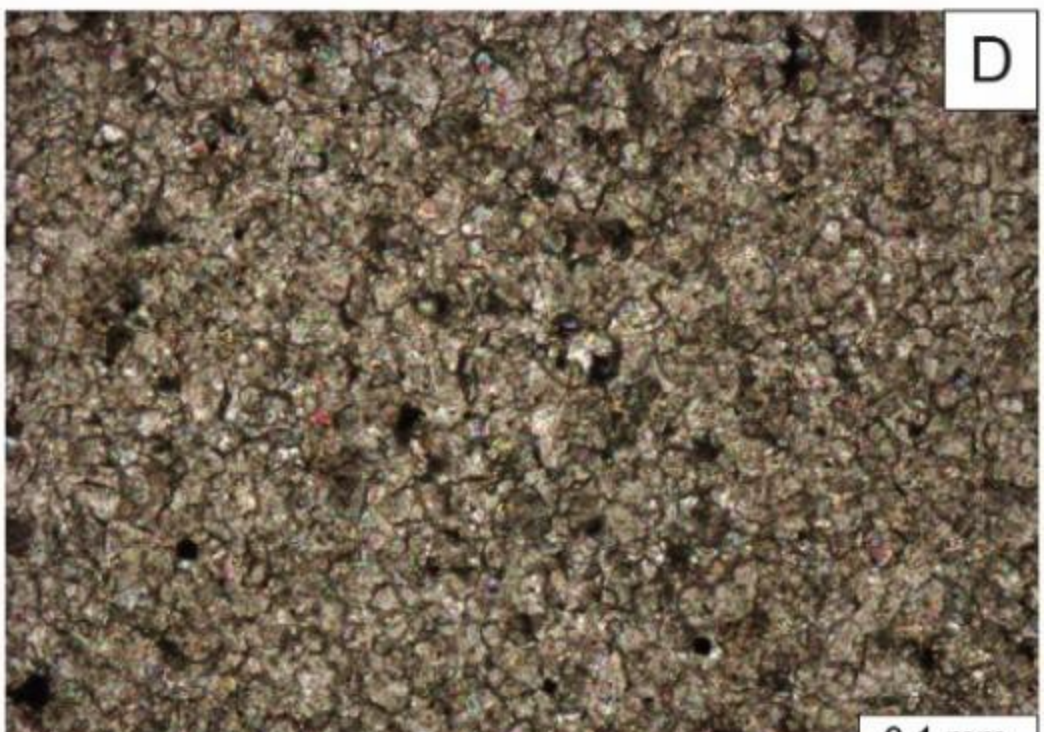
D
0.1 mm

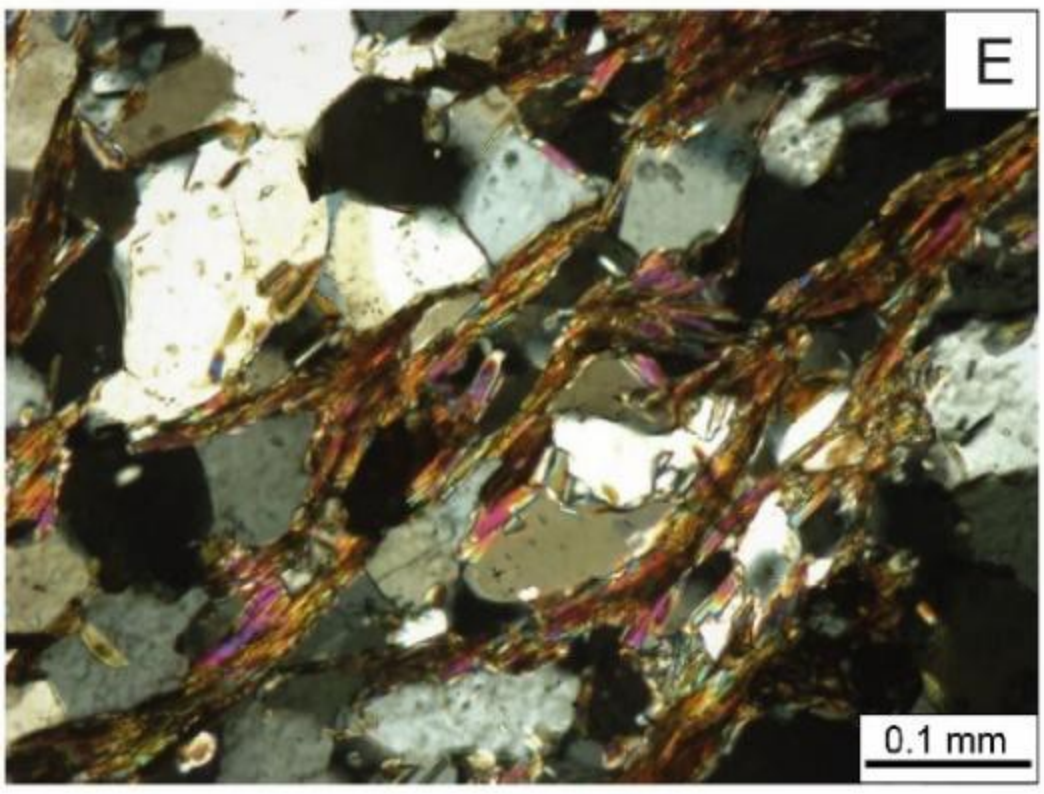
E
0.1 mm

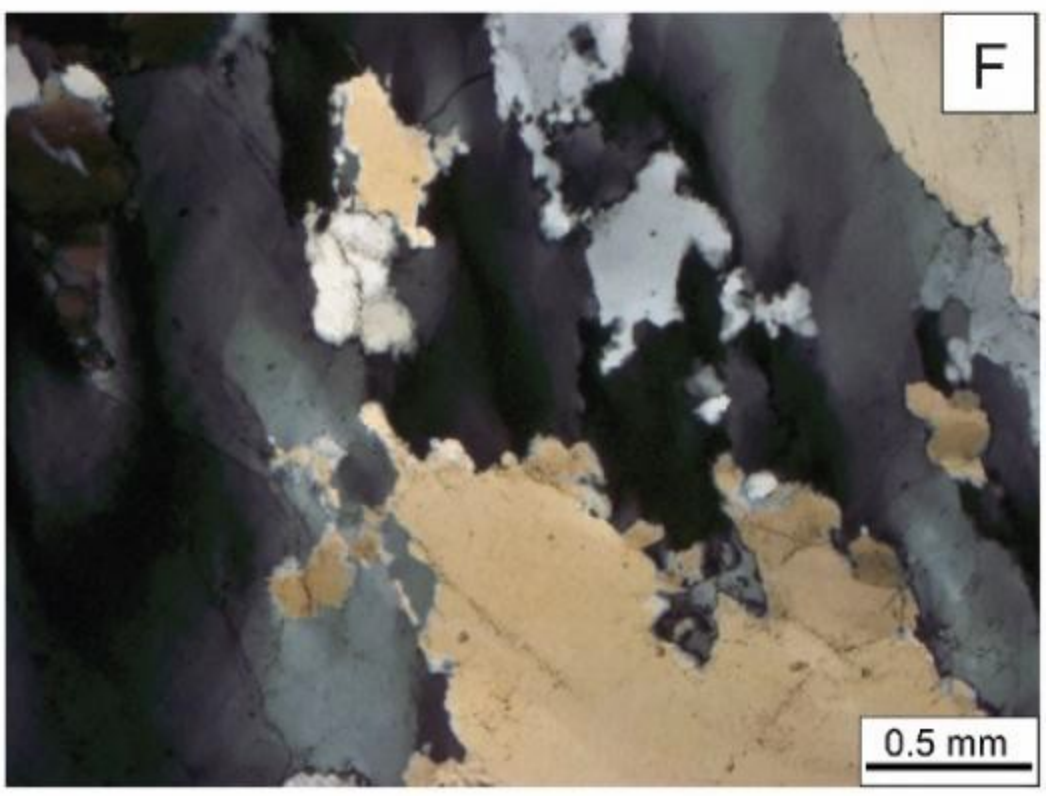
F
0.5 mm

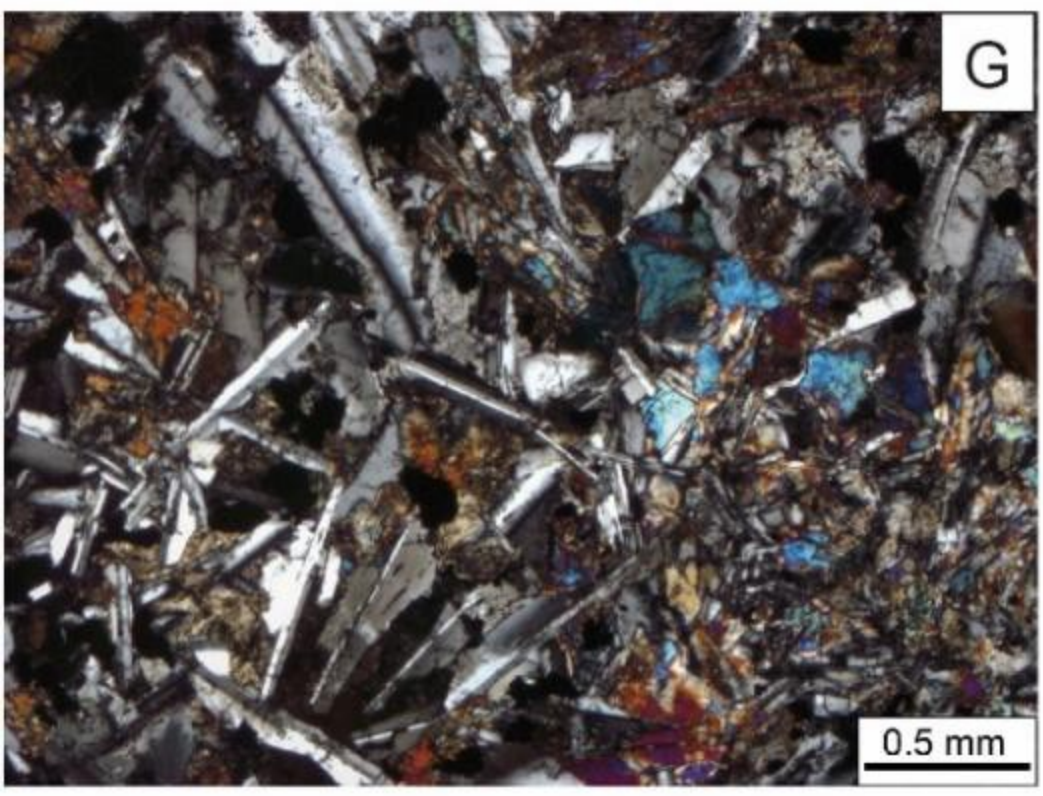
G
0.5 mm

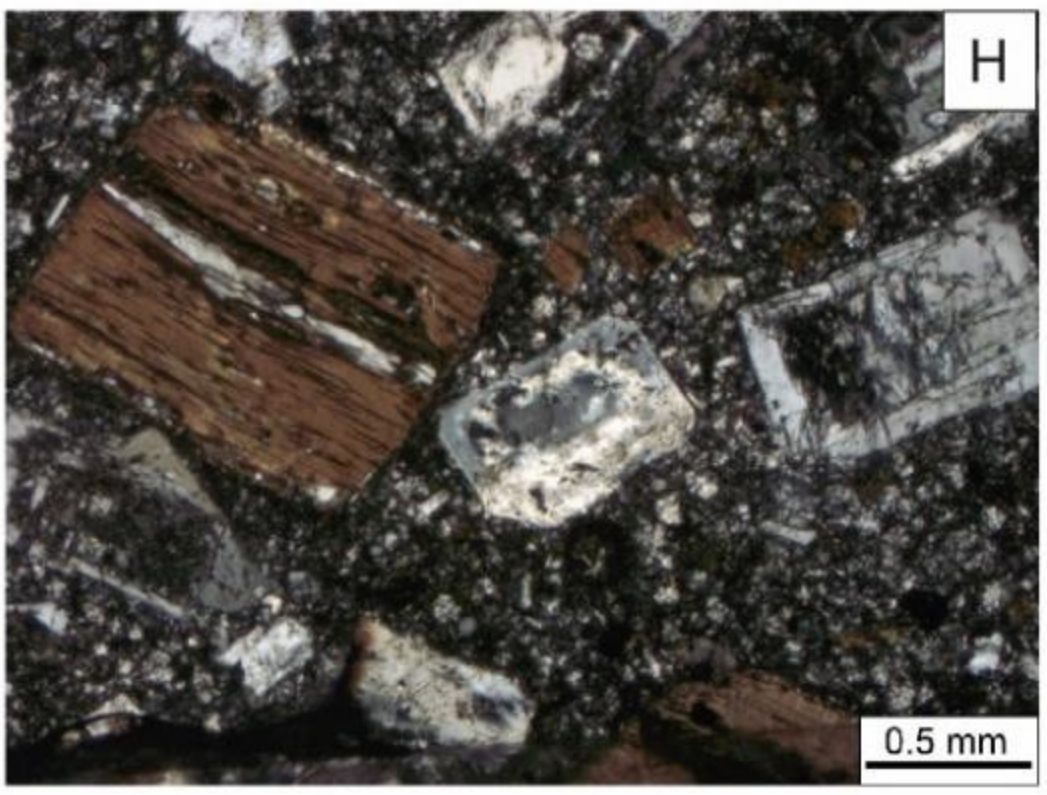
H
0.5 mm

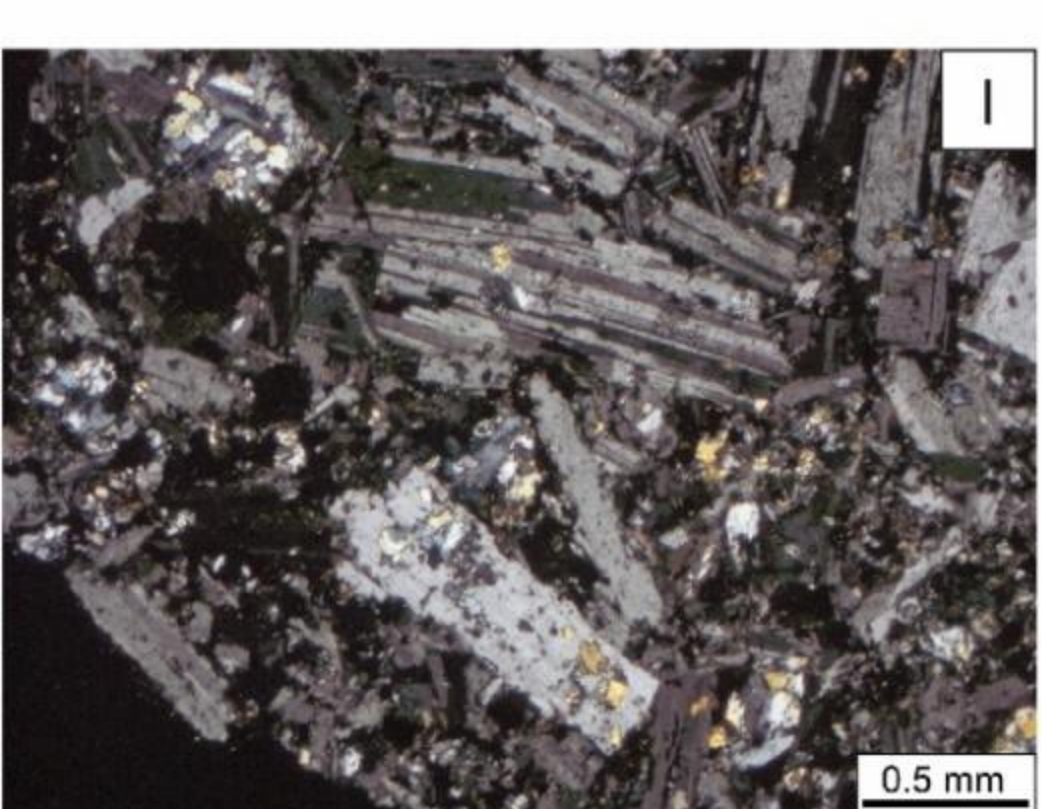
I
0.5 mm

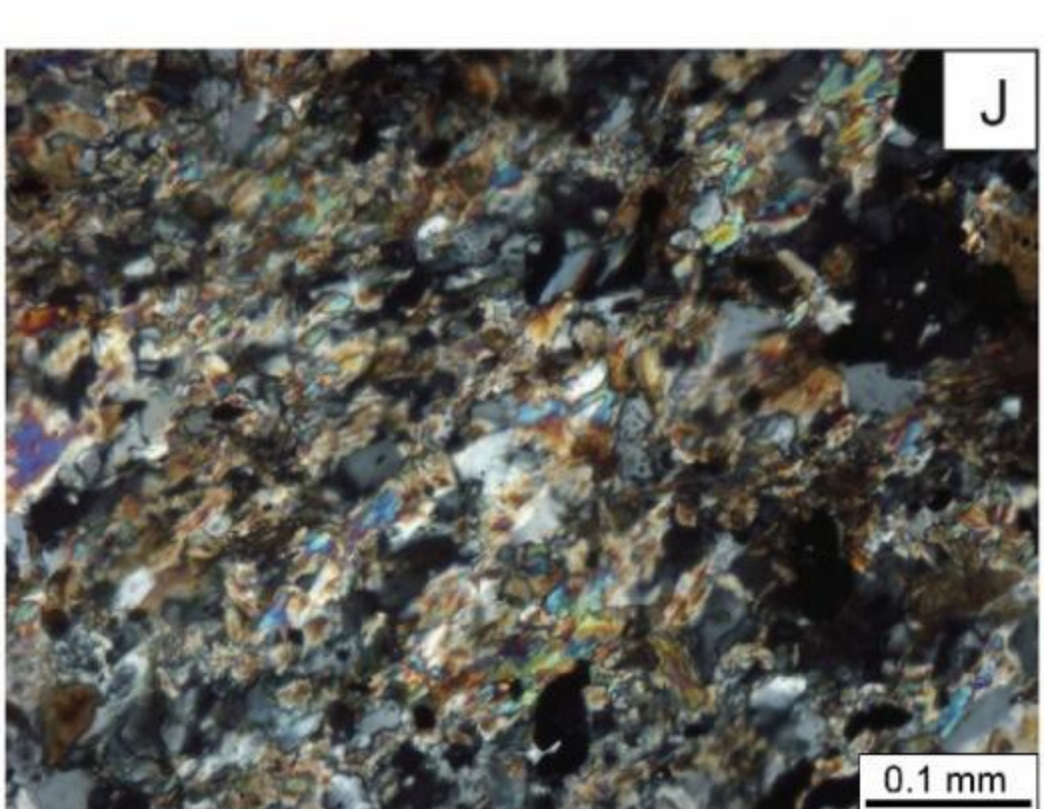
J
0.1 mm

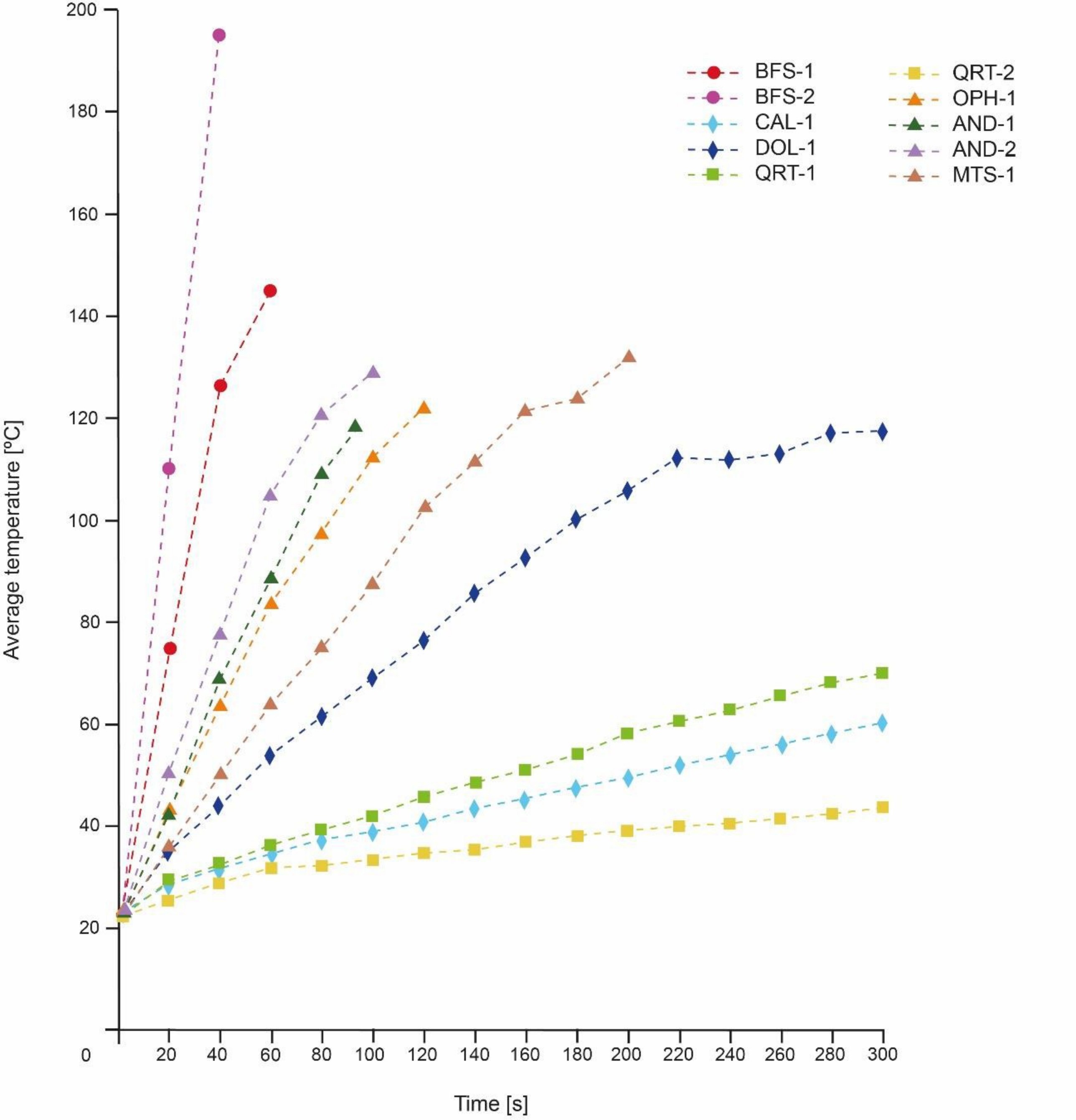
BFS-1
BFS-2
CAL-1
DOL-1
QRT-1
QRT-2
OPH-1
AND-1
AND-2
MTS-1
Average temperature [ºC]
0
20
40
60
80
100
120
140
160
180
200
0
20
40
60
80
100
120
140
160
180
200
220
240
260
280
300
Time [s]

BFS-1	y = 7.8783x + 29.645	R^2 = 0.9617
BFS-2	y = 16.321x + 22.933	R^2 = 0.9998
CAL-1	y = 0.4376x + 26.192	R^2 = 0.9877
DOL-1	y = 1.2146x + 33.74	R^2 = 0.9519
QRT-1	y = 0.5757x + 26.146	R^2 = 0.9908
QRT-2	y = 0.232x + 26.488	R^2 = 0.9357
OPH-1	y = 3.159x + 27.403	R^2 = 0.9858
AND-1	y = 4.1218x + 22.144	R^2 =0.9982
AND-1	y = 4.1191x + 29.299	R^2 = 0.9656
MTS-1	y = 2.1034x + 28.117	R^2 = 0.9818

Average temperature [ºC]

0 20 40 60 80 100 120 140 160 180 200

0 5 10 15 20 25 30 35 40 45 50 55 60 65 70 75 80

Energy Consumption [Wh/Kg]

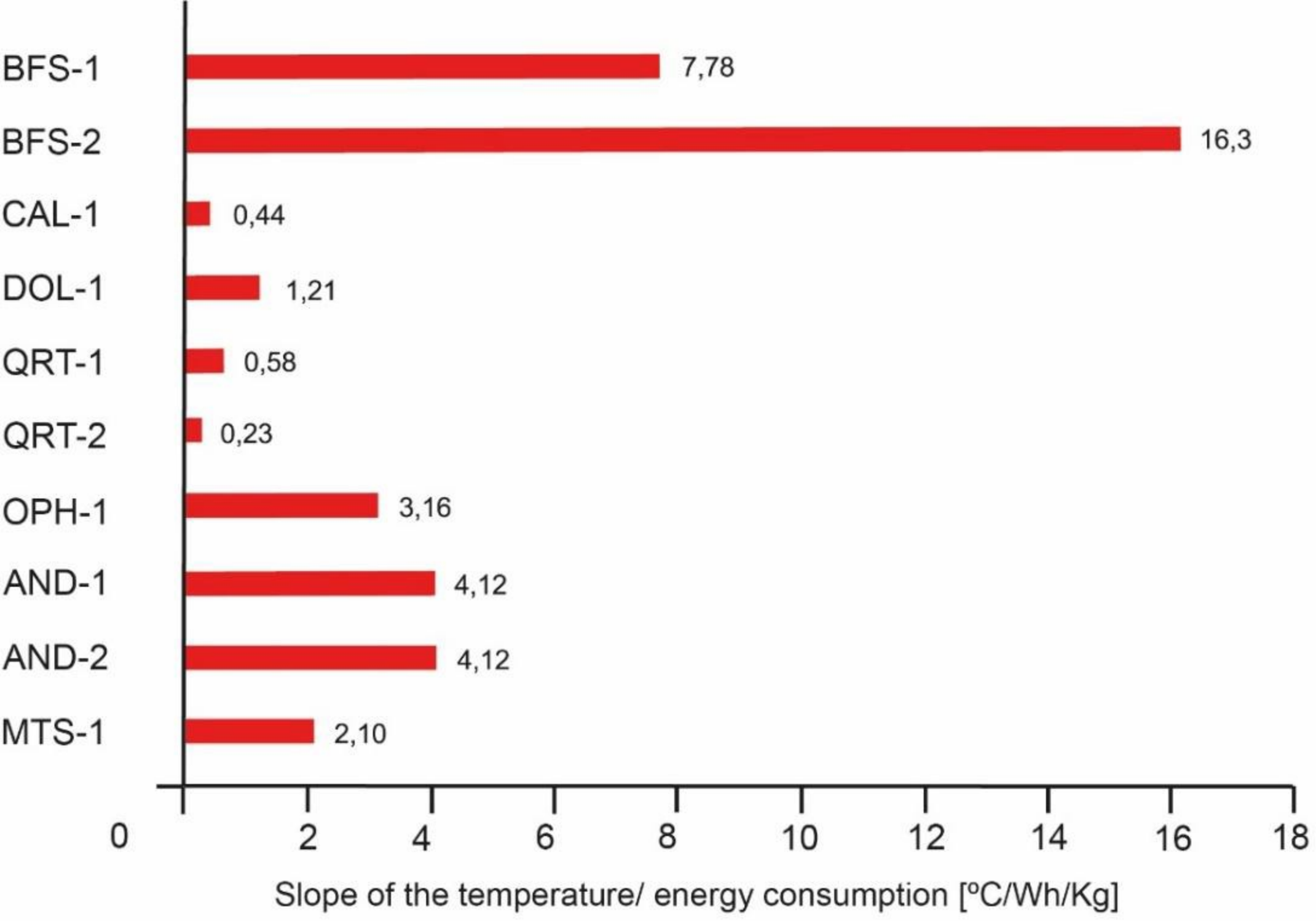
BFS-1
BFS-2
CAL-1
DOL-1
QRT-1
QRT-2
OPH-1
AND-1
AND-2
MTS-1
7,78
16,3
0,44
1,21
0,58
0,23
3,16
4,12
4,12
2,10
0
2
4
6
8
10
12
14
16
18
Slope of the temperature/ energy consumption [ºC/Wh/Kg]

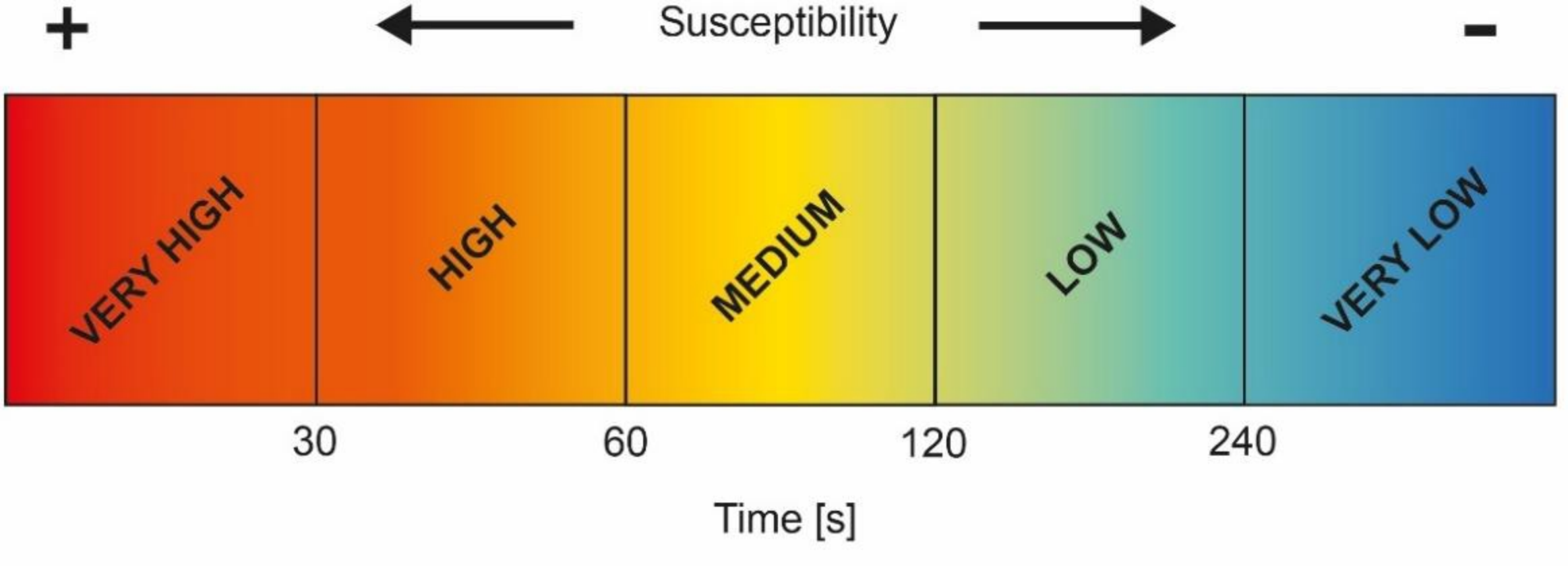
+
Susceptibility
-
VERY HIGH
HIGH
MEDIUM
LOW
VERY LOW
30
60
120
240
Time [s]